4-1 Correlation between Gravity Distribution and Geology

4-1-1 Outline

Isogal lines are concentrical around a negative gravity anomaly south of Bou Mia and with the approximate NE-SW direction as its main direction may be mentioned as a characteristic of the general gravity distribution in this area. As stated already, this characteristic is a strong effect of the Precambrian Crystalline Schists distributed in the Moyen Atlas and Haut Atlas mountains running to the north and south of the surveyed area. Density of the Schists reportedly is about $\rho = 2.7 \sim 2.9$ in the rock density measurement results provided by the B R P M thus it is considerably higher than $\rho = 2.6$ which is a density of the Granites forming the basement in this area.

Pl. II-4((Residual Gravity Map in Polynomial of Second Order)to be referred to hereafter merely as "residual gravity map") obtained from the gravity trend analysis with eliminating these effects from outside the surveyed area is considered to indicate relations between the Granites and the covering sediments. Effects of small Crystalline Schists body deep in the ground still remain in the residual gravity map. We analysed the residual gravity map with taking care of remained effect of deep Crystalline Schists. This effect is the high-gravity anomaly being in the E-W direction about 10 km SSE of Bou Mia at the south end of the residual gravity map.

The following is discussion of how the characteristic gravity anomaly shown in the residual gravity map and the filtered Bouguer anomaly maps are related to the local geology.

4-1-2 Correlation between Gravity Distribution and Formations

The gravity distribution in the residual gravity map is believed to mainly reflect a two-layer structure consisting of the Granites and the Permian and subsequent sedimentary rocks. It should, therefore, be considered that the basement is exposed or hidden at a shallow depth where the residual gravity values are great and the depth of the basement increases with the decrease of residual gravity values rather than considered, that specific formations are correlation with respect to high-gravity parts and low-gravity parts.

But in limited localities, gravity anomalies due to formation difference are known to exist in conjunction with the basement structure or the surface topography. So, their correlation is also discussed hereunder.

(a) In this area, outcrops of basement Granites are known to exist generally at the following two places:

Zayda Granite Body: Small-scale distribution around Zayda and large body widely distributed to the east of Zayda.

Bou Mia Granite Body: Body distributed northwest of Bou Mia and limit -ed by a fault running in the approximate N-S direction.

The edges of both Granite bodies are exposed in the northwest and northeast of the area. In the residual gravity map, high-gravity anomalies are developed where these Granite bodies are. Thus, as stated in "2-3-1 Density Measurements of Rock Samples", the Granites correspond to high-gravity anomaly.

(b) The Granites comprises granite (Gr), contaminated granite (Cnt-Gr), aplitic granite (Ap-Gr) and others distributed in the surveyed area.

The residual gravity map and the filtered Bouguer anomaly maps hardly contain any indications of gravity anomaly due to changes of these rock facies. This is in agreement with the fact that the average density of each rock facies has no significant difference in the rock density measurement results listed in Table II-5.

Therefore, considered that, from the position of gravity survey, these should be handled as one and the same, and they are hereafter referred to simply as "The Granites".

(c) In the density measurement for rock samples, βQ_2 Basalt lava shows the greatest density, the average being 2.78. In the surveyed area, it is not only distributed for about 6 km^2 on the southeastern side of Bou Mia but is also known to exist about 7 km SWW of Zayda sporadically as small-scaled lava flows. But in the various gravity maps, gravity distribution corresponding to these basalt lavas shows no high-gravity anomalies, rather, low-gravity anomaly on the southeast side of Bou Mia.

The βQ_2 Basalt lava distributed in this surveyed area may be so thin that it is not reflected in gravity anomalies.

(d) There is a close correlation between gravity anomaly and geological distribution in parts where, as stated already, gravity distribution is directional in the "Intermediate Wave-Length Bouguer Anomaly Map". In other words, negative gravity anomalies being in the NW-SE direction in the banks of the Agarsif river and the Almagh river correspond to T_1 Mudstone Formation and T_2 Marl Formation while positive anomalies in the similar direction correspond to P-T Red Sandstone Formation or K_{2cm} Mudstone Formation. The negative anomaly continuing in the NNE-SSW direction on the north side of the Ansagmir river mainly corresponds to T_2 Marl Formation.

It is more reasonable to think that this correlationship is caused by the thickness of formations, rather than as the result of density difference of each formation, namely, that high-gravity anomaly is around a lower old formation, such as P-T Red Sandstone Formation, because the Granites are shallow, but that under an upper relatively new formation, such as T_1 Mudstone Formation or T_2 Marl Formation, there are low-gravity anomalies because the Granites are deep.

(e) In the residual gravity map, high-gravity anomaly shown by isogal lines in the E-W direction is at the south end of the surveyed area. This high-gravity anomaly seems to be due to Precambrian Crystalline Schistes which is more dense than the Granites.

It is considered from distributions of Jurassic and Cretaceous sediments that Crystalline Schistes being a basement of the Haut Atlas mountains in the NEE-SWW direction are as if penetrating to the south of the surveyed area. It is presumed that the high-gravity anomaly was formed by the northern projection of this penetration as it was not eliminated by gravity trend analysis.

(f) A large low-gravity anomaly zone is in south to southeast of Bou Mia and the existence of a basin-like structure is presumed there. A high anomaly with relatively short wave-length is known to exist at the center of this structure but, judging from its wave-length, this high anomaly is unlikely a reflection of the basement.

In Fig. II-8 showing geological columns of drill holes in and around the surveyed area, the HM-2 column of about 11 km southwest of Bou Mia shows that a β_{P-T} Basalt Formation lies at the depth of about 330 m to 430 m. This Basalt Formation has an average density of about 2.5, which exceeds the densities of the formations lying above and below it.

From this fact it is presumed that the high-gravity anomaly seen in the above-mentioned low-gravity anomaly zone was caused by β_{P-T} Basalt Formation which has higher density than most other sedimentary rocks lying over the basement.

4-2 Presumed Basement Structure

Pl. II-6 is a contour line map of depth of the basement rock from the ground surface by two-layer structure analysis.

It is the results of the three-dimensional simulation calculations carried out by setting the density difference between the upper and lower layers at 0.2 g/cm^3 and using the value of residual gravity of the second order. It is considered to show the underground depth to the surface of the Granites.

This map is prepared in due consideration of granite outcrops and drill holes. This section explains mainly a basement structure about its depth from the ground surface. The section "4-4 Interpreted Map of Underground Structure" will show a basement structure about its elevation.

The basement structure in this area is presumed from Pl. II-6 (Contour Line Map of Depth of Basement Rock from Ground Surface) as follows:

(a) Outcrops of the Bou Mia Granite Body and Zayda Granite Body are encircled by contour lines of 50~100 m.

The east edge of the Bou Mia Granite Body is indicated by relatively crowded contour lines hinting to a fault-like depression on the east side. Around the Zayda Granite Body, the contour lines are not closed, suggesting that it is covered with sedimentary rocks with a gentle inclination.

(b) Throughout the surveyed area, there is a tendency that in the vicinity of a contour line of 200 m, contour lines are relatively close and the basement depth increases. Similarly, in the southwestern part of the surveyed area there is marked basement inclination about of 500 m to 600 m deep.

If vicinities of these crowded contour lines are considered as boundary lines of basement depths, the depth range to 200 m may be defined as a shallow basement area, the range from 200 m to 500 or 600 m as a medium basement area, and the range beyond 500 or 600 m as a deep basement area.

(c) The main basement structures in the shallow basement area may be generally divided into the following three:

(i) There is an N-S basement axis conforming to the Bou Mia Granite Body at the west end of the surveyed area.

(ii) In the northern part of the area, there is a dominant E-W saddle-like structure, over 6 km in width, continuing from the Bou Mia Granite Body to Zayda via the Agarsif river. The depth increases slowly on the north side of an upheaval of the basement while on the south side it increases steeply.

(iii) In the eastern part of the area, there is a shallow NNE-SSW basement axis running along the Ansagmir river from the outcrop of the Zayda Granite Body.

(d) Meanwhile, a basin-like depression of over 600 m deep is developed southeast of Bou Mia with a maximum depth of about 980 m.

Contour lines indicating an E-W basement upheaval are distributed in the middle of this depression. These do not show the basement depth itself; the presumed cause is a density anomaly somewhere above the surface of the basement.

(e) NW-SE contour lines run along the Agarsif river and the Almagh river in the northwestern part of the surveyed area and crowded contour lines appear at several places. The basement is shallow around both rivers and deep on banks of them.

It is, therefore, necessary for the local basement structure to be considered in terms of basement contour lines converted into elevations above sea level.

4-3 Profiles of Underground Structure

Profiles of underground structure were prepared by carrying out two-dimensional simulation calculations using residual gravity values on three sections: A-B (Pl. II-7), C-D (Pl. II-8) and E-F (Pl. II-9), which are indicated in each gravity map. Sections A-B and C-D are made to agree with geological sections 4-4' and 2-2', respectively.

Each plates show cross-sections in the following order:

(a) Bouguer anomaly section ($\rho = 2.5$): It is accompanied by a gravity trend section of the second order.

(b) Residual gravity section in polynomial of second order: It is accompanied by the results of two-dimensional simulation calculations at intervals of 250 m as estimated gravity values.

(c) Wave-length Bouguer anomaly section: Short wave-length and intermediate wave-length Bouguer anomalies are indicated as Noise and Normal, respectively.

(d) Two-layer structure section: The results of two-dimensional calculations are indicated by the boundary line between each layer with their densities, and a third layer is also used, if necessary. The results of three-dimensional simulation calculations performed with the density difference of $\Delta\rho = 0.2$ (contour line map of depth of basement rock from ground surface) are also given.

(e) Geological structure section: A geological structure section was prepared, based mainly on the basement structure obtained from the above simulation calculations and taking the various gravity profiles, horizontal interpretations and geological informations into consideration. The basement depression shown in the below-described interpreted map of underground structure are also used here and described under the definition of fault-like step structure.

Each profile is on a scale of 1/50,000 but the vertical scale for (d) two-layer structure section is 1/20,000 and that for (e) geological structure section is 1/10,000.

Hereunder are the estimates of underground structure in the various profiles.

4-3-1 A-B Profile (Pl. II-7)

The A-B profile is set in the E-W direction in conformity with the saddle-like structure of the basement on the north side of the surveyed area. It mainly is to show depth of the shallow basement and to detect depression on the basement reflecting the N-S low-gravity anomaly that orthogonally crosses the section.

The main surface geological distribution at this section consists of outcrops of the Granites, the basement rock in this area, at both ends of the section and in the vicinity of the Moulouya river and P-T Red Sandstone Formation, K_{2cm} Mudstone Formation, K_{2t} Limestone Formation and T_1 Mudstone Formation that cover the basement, from bottom upward in the order of mention. Faults are known to exist in the vicinity of granites outcrop at the west end of the section. In this vicinity, drastic gravity changes are noted from the various gravity sections also.

In the residual gravity section in polynomial of the second order, gravity variation are, indeed, small, for only about 2 mgal from +2.5 mgal to +0.5 mgal. It is characteristic that the above-mentioned granites outcrop is reflected in a high-gravity anomaly.

The following underground structure is presumed from the geological structure sections resulting from the analysis.

(a) A fault-like basement structure F-①is presumed on the east side of the Bou Mia Granite Body outcrop at the west end of the section. From the findings in a geological survey, several faults are known to exist in this vicinity. It is considered, therefore, that this fault-like step structure F-①represents a basement activity in which, rather than cause a monotonous throw, depth is gradually increased in several steps in the vicinity of this structure.

This fault-like step structure F-① is vertical and seems to affect the sedimentary rocks above.

(b) The basement lies shallow underground at depths of 0 to about 200 m. Particularly east of the above-mentioned fault-like step structure, a more or less horizontal basement structure lies at about 1,450 m above sea level.

(c) Underground of the Route P21 and the station No. 173, there clear are channel-like grooves on the Granites and the deepest parts of them are believed to be about 150 m and about 200 m underground.

Besides them, several gentle depressions seem to be near the center of the section.

4-3-2 C-D Profile (Pl. II-8)

The C-D profile is in the N-S direction passing through the vertical drill hole HM-1 carried out in the surveyed area.

The main surface geological distribution at this section consists of the K_{2cm} Mudstone Formation, T_1 Mudstone Formation and Q_1 Siltstone Formation, from bottom upward, distributed from the northern end of the section to southward. Partially, there are βQ_2 Basalt lava jutting out in the northern part of the section and Q_3 River sediments along the Moulouya river. The area south of the Moulouya river and its vicinity representing about 2/3 of the section is widely covered by Quaternary sediments. Further south of the section, Precambrian Crystalline Schistes are known to exist.

In the residual gravity section of the second order, residual gravity values, with the high-gravity anomaly of about +1.5 mgal north of the section as the peak, decrease gently on the north side and rather abruptly on the south side. The minimum residual gravity value of -1.3 mgal is registered near the station No. 134. Further south, the values gently rise again up to the south end of the section. In wave-length Bouguer anomaly sections, variation on gravity values is so small that structural change is hardly seen at shallow depths.

The following underground structure is presumed from the geological structure section resulting from the analysis.

(a) In the northern part of the section, an anticline structure of the Granites lies underground with its apex at about 100 m from the ground surface, and its altitude lowers toward both north and south.

(b) Underground in the vicinity of Route P33, there is a basement depression to the southward controled by a fault-like step structure F-②.

(c) South of the Moulouya river, the basement depth is estimated about 300~500 m from the ground surface. This, in terms of elevation above sea level, is flat at about 1,100 m, showing a horizontal basement structure for a large area.

The sedimentary rocks covering the Granites within this area are believed to be conformable and horizontal.

(d) The Precambrian Crystalline Schists being at deep of the southern end of the section seems to vertically adjoin the Granites and form the basement further south of the section.

4-3-3 E-F Profile (Pl. II-9)

The E-F profile is in the NE-SW direction, the direction connecting the high-gravity anomaly zone and the low-gravity anomaly zone in the residual gravity map, for the purpose of assessing the general basement structure and the depths thereof in the surveyed area.

The main surface geological distribution at this section consists, in the northeastern half of the section, of P-T Red Sandstone Formation, K_{2cm} Mudstone Formation and T_1 Mudstone Formation, Q_1 Siltstone Formation and Q_2 Siltstone Formation accumulate in that order. In some parts, βQ_2 Basalt Formation and Q_3 River sediments are also distributed; these formations are relatively new, compared with the northeastern half.

In the residual gravity section of the second order, this section is divided into two general areas, the high-gravity anomaly zone with residual gravity values of +1.8 mgal ~ +1.0 mgal on the northeast side of the Agarsif river and its vicinity and the low-gravity anomaly zone with residual gravity values of -3.0 mgal ~ -4.1 mgal on the southwest side of the Moulouya river and its vicinities. A remarkable gravity gradient with a difference of 4 ~ 5 mgal exists in the middle part of the section located between these two rivers. In the intermediate wave-length Bouguer anomaly section, characteristic positive anomaly was at three points: vicinity of the station No. 665, vicinity of the station No. 49, and vicinity of the station No. 840, hinting disturbance of underground structure in vicinities.

The following underground structure is presumed from the geological structure section resulting from the analysis.

(a) In the northeastern half of the section, an anticline structure of the Granites lies underground near the station No. 665 with its apex at a depth of about 80 m. This structure gently decreases in altitude on the northeastward.

(b) On the southwest side of this anticline structure, the Granites sharply descends, controled by two fault-like step structures F-② and F-④. The displacement is particularly remarkable at F-④ with a throw of several hundred meters.

(c) In the middle part of the section where the fault-like step structures F-② and F-④ exist, the Granites undulate greatly. It is presumed that, in the vicinity of the station No. 49, a domed apex of the Granites lies about 100 m from the ground surface.

(d) On the southwest side of the Moulouya river and its vicinity, the basin-like structure to which reference has been repeatedly made so far is known to continue for more than 8 km. This basin-like structure consisting of a depression in the Granites reaches down to 600m ~ 800m underground and its altitude is about 800 to 900 m.

(e) It is presumed that this basin-like structure is covered by P-T Red Sandstone Formation, βP-T Basalt Formation, J_1 Limestone Formation, T_1 Mudstone Formation and Quaternary sediments, from bottom upward, which accumulate conformably and thickly.

(f) In the two-layer structure section, III (ρ = 2.58) was analysed as a third layer. This was interpreted to be a part dominated by high-density basalt contained in the βP-T Basalt Formation and indicated with oblique lines in the plate.

4-4 Interpreted Map of Underground Structure

Before discussing the underground structure in the surveyed area, it is necessary generally to describe the basement structure in the area with its surroundings.

The basement in the surveyed area is Granites but the basement around the Moyen Atlas mountains north of the surveyed area and Haut Atlas mountains south of the surveyed area is considered to be Precambrian Crystalline Schists. The relationship of these basement rocks is clear in Fig. II-10 and the gravity trend section of the second order in Pl. II-8. In other words, mainly the gravity distribution in Fig. II-10 seems to be reflected relation between the Crystalline Schists and the Granites. Similarly, gravity distribution shown in the gravity trend of the second order is believed to reflect general structure of the Crystalline Schists. (See Fig. II-13)

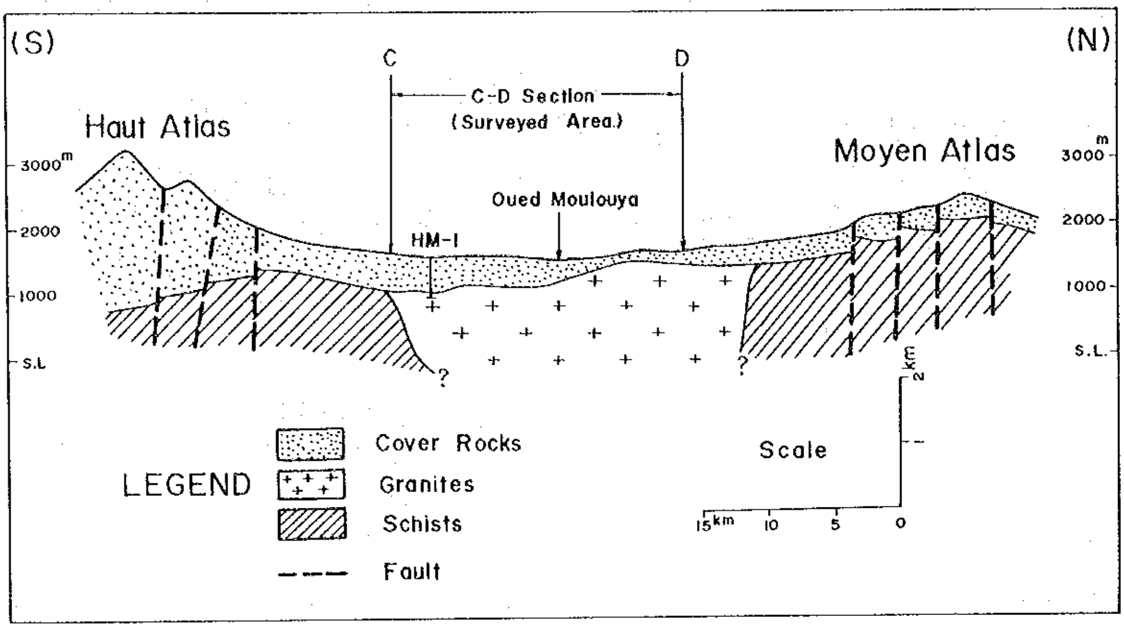

Fig. II-13 Schematic Profile of Basement Structure

The type profile is sketched along the underground structure profile C-D, and clearly shows structure of the Granites and Schists that form the basement.

In Fig. II-10, great low-gravity anomaly developed in the surveyed area located between the Moyen Atlas mountains and the Haut Atlas mountains is presumed to be due mainly to location and scale of the Granites protruding into the Crystalline Schists as well as to the density difference between them. Judging from regional gravity distribution, the Granites seems to be distributed as a so-called stock vertically contacting with the Crystalline Schists on both edges and distributed only limitedly in the depths.

Thus the basement in Haute Moulouya Region is the Granites in the surveyed area and Crystalline Schists outside the surveyed area.

Pl. II-10 is an underground structure map. In it, the results of general analysis are indicated as contour lines of basement rocks, fault-like step structure, paleochannels, etc. and numbers are assigned to structures whenever necessary.

The details are as follows:

4-4-1 Contour Lines of Basement Rock

Contour lines of basement rock in Pl. II-10 were obtained by converting basement depths in Pl. II-6 into elevations above sea level using station elevations and may be considered to show elevations on the surface of the Granites.

Naturally, the basement structure indicated by basement contour lines closely resembles the basement structure indicated by basement depth in Pl. II-6. However, there are some differences in the northwestern and southwestern parts of the surveyed area where topographical changes are great.

The underground structure presumed from the basement contour lines is as follows:

(a) The axial direction of the Granites extending along the Ansagmir river from the Zayda Granite Body generally agrees with the NE-SW direction of the fault-like structure known in the east of the surveyed area. Thus, there is a structure line in this direction. Similarly, N-S structure line is presumed to exist at the eastern edge of the Bou Mia Granite Body.

(b) The saddle-like structure of the basement that runs in the E-W direction in the northern part of the surveyed area connecting the Zayda Granite Body and Bou Mia Granite Body is generally flat at an elevation of about 1,450~1,500 m with some small irregularities. Thus this saddle-like structure is important since it presumably serves as a watershed dividing the paleochannels into northern and southern parts.

Main formations covering this E-W saddle-like structure are Permo-Triassic P-T Red Sandstone Formation and Tertiary T_1 Mudstone Formation and T_2 Marl

Formation. Besides, Cretaceous formations are on the north side of this structure while, on the south side, a Jurassic J_1 Limestone Formation is accumulated.

(c) A basin-like structure indicated by contour lines of elevations not exceeding 1,000~1,100 m is in the southeast of Bou Mia. In its center there is an elevated portion indicated with oblique lines in the underground structure map. This probably was caused by high density a β_{P-T} Basalt Formation.

Namely, it is considered that the basement forming this basin-like structure is relatively flat and that the P-T Red Sandstone Formation, β_{P-T} Basalt Formation, J_1 Limestone Formation, T_1 Mudstone Formation and Quaternary sediments that accumulate over the basement are nearly horizontal and thick.

Elevation difference between this basin-like structure and its vicinity where the basement is exposed or located at a shallow depth is more than 800 m, at the maximum. Basement structure is presumed from the geological distribution mentioned in (b) to have been formed in the old Pre-Jurassic period.

(d) Areas where the basement is shallow are places with clear correspondence between a specific formations and the irregularities on the surface of the basement.

Surface indication of depression of the basement are belt-like groove extending in the NNE-SSW direction on the north side of the Ansagmir river and parallel depressions running in the NW-SE direction on the south banks of the Agarsif river and the Almagh river. At these position, Neogene T_2 Marl Formation is on the ground surface and is believed to be thick over the basement.

Meanwhile the P-T Red Sandstone Formation distributed along the Agarsif river and the Almagh river on the east side of the Bou Mia Granite Body are over concaves of the basement. A dome-like structure of the basement seems to exist under P-T Red Sandstone Formation where the down stream of the Almagh river crosses the route P33.

4-4-2 Fault-like Step Structure

It is known from the results of the geological survey that, in the surveyed area, faults running in the N-S or NE-SW direction exist in the vicinities of the Bou Mia Granite Body and Zayda Granite Body. Since, however, relatively new formations not dating beyond the Tertiary period cover most of this gravity surveyed area, many parts of local fault structures remain to be clarified.

Steep depressions in the basement were continuously assessed from the view-point of gravity survey and presented in the underground structure map as "fault-like step structure". This fault-like step structure is a terminology referring generally to broad vertical motion involving a relatively steep slope accompanied by a fault and occurring in several steps rather than a monotonous throw occurring all at once.

The fault-like step structure F-① shown in the underground structure map (it will be referred to hereafter simply F-①) generally agrees with the N-S fault limited by the eastern edge of the Bou Mia Granite Body. The Bou Mia Granite Body is believed to increase gradually in depth toward the east, with this fault as the boundary, and this step structure seems to be represented by F-①.

The basement structure in the surveyed area may be generally divided by the boundary lines into three fault-like structures, that is, F-①, F-② and F-③ and three boundary lines: F-④, F-⑤ and F-⑥. In the vicinities of these two sets of boundaries the basement structure shows not only the difference of basement depths but also the difference of sedimentary environments, but it is presumed from the surface geological distribution that the present basement structure will retain Pre-Triassic topography.

Thus the change of geological environments can be presumed from the existence of a fault-like structure and, at the same time, it may be possible to discuss specifically where to prospect in the future and to pin-point likely ore deposits.

The structure F-⑥, as stated at the beginning of this section, is presumed to show boundary surface where the Granites on the north side and the Crystalline Schists on the south side meet deep underground. It is considered, therefore, that the basement contour lines indicated in this vicinity show not only basement elevations but other factors as well.

4-4-3 Presumed Paleochannels

Paleochannels are presented in the underground structure map by tracing continuous grooves on the basement and indicating their positions and directions with arrows. In finding these paleochannels, mainly the basement contour line map was used, and the Bouguer anomaly map, the residual gravity map of the second order, and the filtered Bouguer anomaly maps were put together with it, and only what was derived from them all was subjected for estimation.

The Main paleochannels are generally the following four.

(i) A paleochannel comprising a main stream marked C-① and extending for more than 10 km and its tributaries.

(ii) Paleochannels comprising mainly streams marked C-② and C-③ which flcw south from the east side of the Bou Mia Granite Body and join together east of Bou Mia.

(iii) Paleochannels represented by C-④, C-⑤ and C-⑥ and tending to be dispersed to the south and north from the watershed of the E-W basement.

(iv) Paleochannels at the southeast end of the surveyed area. Its main stream is C-⑦ and joins with the tributaries in the east.

These are all known to exist in areas with shallow basement depths, the maximum depth being 500 m. This does not mean that no paleochannels exist at great depths but that, whereas basement irregularities at shallow depths are reflected as gravity anomalies, those at great depths are not reflected as gravity anomalies.

Flow directions of paleochannels were determined from the elevations in paleotopography indicated by basement contour lines. Since, however, there is a great time gap between the paleotopography of today and the start of these paleochannels, the actual flow directions of the paleochannels may be somewhat different, depending on basement movements and other factors.

Paleochannels given as underground structures may be described separately by characteristics as follows:

(a) C-① which is the largest in the surveyed area and a paleochannel detected at shallow depths not exceeding 100 m in the area ranging from Zayda to southwest of Zayda may be mentioned as gently sloped paleochannels.

The former flows southward with gentle slope of about 15 m/km at its upper and middle streams, turns southwest, and disappears at great depths. On its east bank, C-① has several tributaries, reflecting that it contained much water.

With regards to the latter, poleochannels south-flowing C-④ and C-⑥ and flowing north in parallel were detected. The north-flowing paleochannels are yet to be completely clarified since they are at the north end of the surveyed area. However, they will be clarified as the survey extends northward in the future.

(b) Paleochannels known to exist at relatively great depths, deeper than the fault-like structures F-② and F-③, and flow into a basin-like structure southeast of Bou Mia and paleochannels typified by C-⑦ at the southeast end of the surveyed area may be mentioned as steeply sloped paleochannels.

(c) As paleochannels tending to meander, there are C-①, C-⑥ and paleotopography continuing downstream from C-②.

(d) As paleochannels forming basement depressions where water gathers, there is the central part of C-②. Also, the gently sloped parts of C-① and C-⑥ involve such possibilities.

4-5 Presumption of favorable zone for mineralizations

The surveyed area has not only lead ore deposits such as a mine in Zayda which is in operation but also ore indications of uranium. Thus this survey is expected to bring more promises as a mining district.

The lead ore deposit at the Zayda mine is in a arkose sandstone bed at the base of a P-T Red Sandstone Formation. Lead-containing mineral were precipitated as lead-containing solution infiltrated the arkose sandstone at the time of its solidification. Hence, the lead deposit has close relations with the paleochannel topography.

As local uranium ore indications, geological survey in and around the gravity surveyed area has revealed the existence of four types: vein-like type, sandstone type, carapace type and conglomerate type. Of these, the sandstone type believed to be directly related to the basement structure is discussed below.

Uranium ore indications of the sandstone type related to arkose sandstone being in a P-T Red Sandstone Formation are closely related to paleochannel topography as well as lead deposits. Uranium originated from Granites in the hinterland is redeposited by the medium of the paleochannel into arkose sandstone contained in the P-T Red Sandstone Formation covering the Granites. Paleochannel topography plays an important role as a topographical environment of uranium deposition and concentration. Not only position and flow direction of paleochannels but also the following conditions are necessary for the deposition of uranium.

(i) Uranium ore indications of Granites, as a source of uranium.

(ii) Sedimentary environments and such geological environments as the lithofacies of terrestrial sedimentary rocks.

(iii) The existence of reduction and settlement of uranium at such places as pools along paleochannels and meander stagnations, where channel water containing resolved uranium can settle and percipitate the uranium.

It is presumed that favorable environments for depositing uranium result from interaction of these conditions.

As seen above, paleochannel topography in the surveyed area, specially gentle slopes, meanders, and pools, is likely to percipitate lead and uranium deposits.

The following areas in the underground structure map may be mentioned as areas in paleochannels that satisfy these conditions.

(a) Approximately 5 km stretch from the upper to the middle stream of the paleochannel C-① extending for more than 10 km south of Zayda, and the end part in its downstream.

(b) The paleochannel C-⑥ formed at shallow depths about 5 km SSW of Zayda.

(c) The center of the paleochannel C-② adjoining the Bou Mia Granite Body about 6 km north of Bou Mia.

Besides, some examples have been reported that uranium is deposited at places far away from hinterland due to other factors than teristics of paleochannel topography.

For example, paleochannels in the area between fault-like structures F-② and F-③ on the one hand, and F-④ and F-⑤ on the other (see the underground structure map), are rather steep but river systems of a relatively recent period do not necessarily flow over paleotopography. On the contrary, water in these systems may flow as subterranean water, infiltrate certain layers, join with water from other channels, and percipitate uranium concentrations. At this point, however, only certain parts in paleochannel topography around shallow basements are noted and hereby mentioned as likely ore deposits for immediate exploration.

Chapter 5 Conclusion

5-1 Consolidated Survey Results

Gravity distribution in Haute Moulouya area in the Kingdom of Morocco has been clarified and the underground structures have been presumed, based on the results of gravity survey conducted for an area of about 400 km^2. Further, leveling results and rock density data have been obtained with the gravity survey.

The analysis carried out on the basis of a Bouguer anomaly map with its corrected density ($\rho = 2.5$) has clarified the geological structures in the surveyed area, as shown in the appended underground structure profile and underground structure map.

The results of the gravity survey may be summarized as follows:

(a) In the surveyed area, Bouguer anomaly values approximately range from -110 mgal to -130 mgal. These negative Bouguer anomalies show the existence of isostasy around the Atlas Mountains.

(b) The Moyen Atlas mountains and the Haut Atlas mountains run in the directions of NE-SW and NEE-SWW, respectively, the north and the south of the surveyed area. The Granites, the basement in the surveyed area, is penetrating into Precambrian Crystalline Schists which is the basement of both mountain ranges. A large circular low-gravity anomaly is a reflection of density difference of these two basement rocks. The surveyed area is at the center of the low-gravity anomaly zone.

(c) It is mainly the basement Granites that reflect high-gravity anomalies. The basement structure was clarified in the basement contour line map from quantitative analysis, and geological structures and paleochannels were presumed as described below.

(d) In the northeastern part and at the northwest end of the surveyed area, outcrops of the Zayda Granite Body and Bou Mia Granite Body are known to exist. Now, a saddle-like structure running almost horizontally in the E-W direction has been found at shallow depths between the two Granite Body. This saddle-like structure seems to have served as a watershed in the paleotopography and to control flow direction of paleochannels.

Similarly, a shallow basement structure running in the NNE-SSW direction has been found along the Ansagmir river in the eastern part of the surveyed area.

(e) A basin-like structure reaching depths of 700~900 m is known to exist southeast of Bou Mia. The sedimentary formations over this structure are nearly horizontal and presumed partially to be intruded by a β_{P-T} Basalt Formation. The depression from the granite outcrops to this basin-like structure is more than 800 m, at the maximum, and there seem to be roughly two steps of depression before reaching great depths.

(f) Belt-like grooves considered to represent paleochannels have been discovered on basements at depths of up to about 500 m. Particularly remarkable points of them are the following:

(i) A paleochannel running southward for more than 10 km is in the south of Zayda. It has a relatively gentle slope and is known to have sporadic meanders.

(ii) Several paleochannels running southward or northward exist at shallow basement depths not exceeding about 100 m in the area from Zayda to the southwest of Zayda.

(iii) Parallel paleochannels are on both banks of the Almagh river on the east side of the Bou Mia Granite Body in the north of Bou Mia and a pool is known partially.

(g) Of the known uranium ore indications in and around the surveyed area, uranium ore indications of sandstone type related to the arkose sandstone of the P-T Red Sandstone Formation is believed to be closely related to the above-mentioned paleochannels.

If gentle slopes or meanders in paleochannels are to be noted as topographically desirable environments for deposition and concentration of uranium, the followings may be mentioned as likely uranium deposits.

(i) The approximately 5 km stretch from the upper to the middle stream of the paleochannel extending for more than 10 km south of Zayda, and the downstream.

(ii) The paleochannel believed to exist at shallow depths about 5 km SSW of Zayda.

(iii) The center of the paleochannel adjoining the Bou Mia Granite Body about 6 km north of Bou Mia.

(h) In the vicinity of Zayda, there are many lead deposits being operated by the Zayda mine management. These are stratiform sandstone-type deposits mineralized in arkose sandstone. With respect to environmental formation they seem to be related to the above-mentioned uranium ore indications of the sandstone type. In other words, the lead deposits exist relatively near the granite body and uranium ore deposits may have developed along extension of the paleochannels on which the lead ore deposits are. Thus, exploring of paleochannels is important for prospecting both minerals.

5-2 Guidelines on Future Exploration

The recent gravity survey has resulted in generally clarifying the basement structure and presuming paleochannels left on the paleotopography as major targets of the survey and thus proved to be successful. Particularly, it has clarified paleochannels at shallow depths and located likely deposits of uranium and lead ores.

From the results of this gravity survey, the following may be given as guidelines on future exploration.

(a) Gravity anomalies reflecting paleochannels on the basement show very small values not exceeding 1 mgal. Therefore, very precise measurement and correction, such as used in the recent survey, is required in future survey. It is desirable for surveying station locations, depending on circumstances.

(b) Since gravity response is remarkable in areas with relatively shallow basement area, areas presumably with deep basement should be excluded from future gravity survey.

(c) In the survey, 600 stations were set for an area of about 400 km^2 ; thus the station density was 1.5 stations per square kilometer. But a higher station density is desirable if small paleochannels at shallow depths are expected to be detected. If, for example, an area of 400 km^2 is to be set up in a district with a maximum basement depth of about 500 m, inter-station intervals of about 400 m and a total of about 900 stations will be required for the survey.

(d) Several paleochannels running northward from an saddle-like basement axis in the E-W direction are estimated to exist in the northern part of the surveyed area. To trace them and select likely ore deposits, survey should be extended to the north.

(e) Confirmatory hole should be drilled in and around the places that have been pointed out as favorable ore deposits. Any gravity survey to be planned for the future may as well involve structural drilling designed to confirm basement depths.

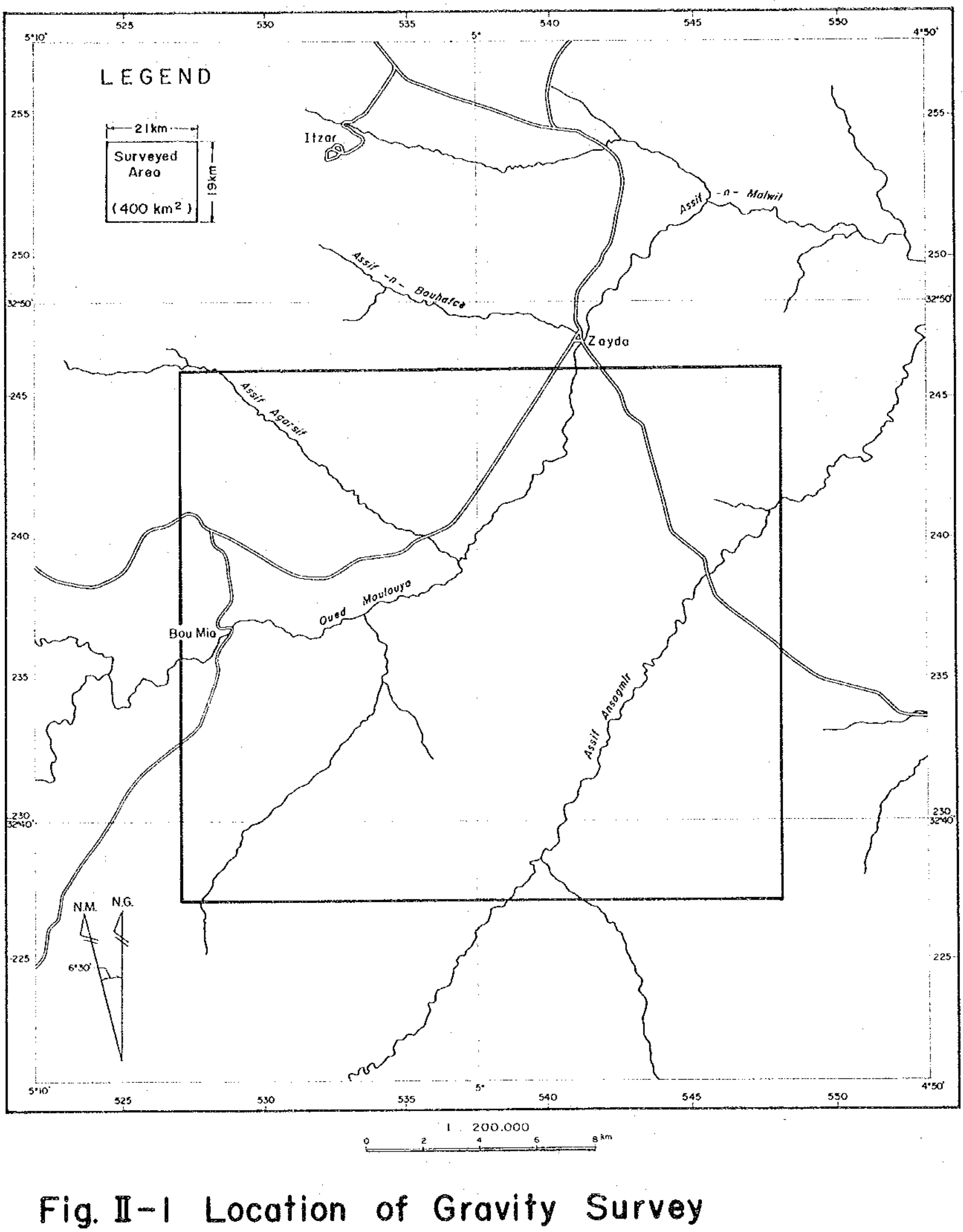

Fig. II-1 Location of Gravity Survey

Station No.	B − 7	X = 540 840 m
		Y = 246 990 m
g = 979,154.65 mgal		Z = 1458.78 m (Altitude)

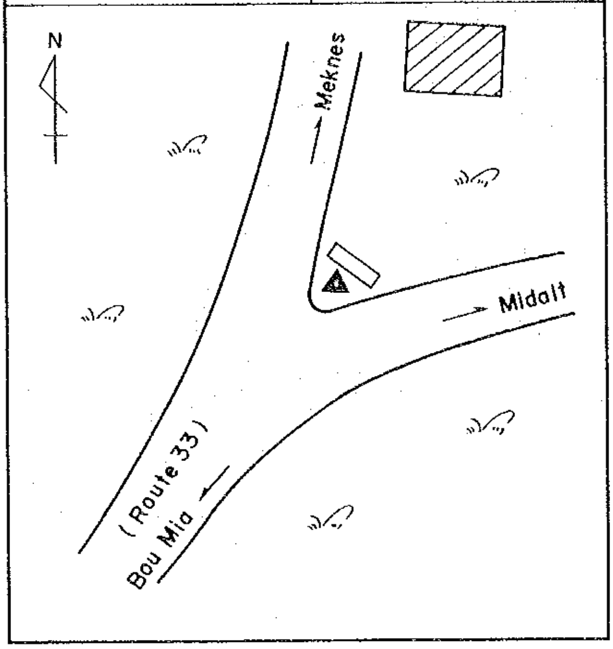

Station No.	B − 8	X = 531 553 m
		Y = 260653 m
g = 979,116.73 mgal		Z = 1801.92 m (Altitude)

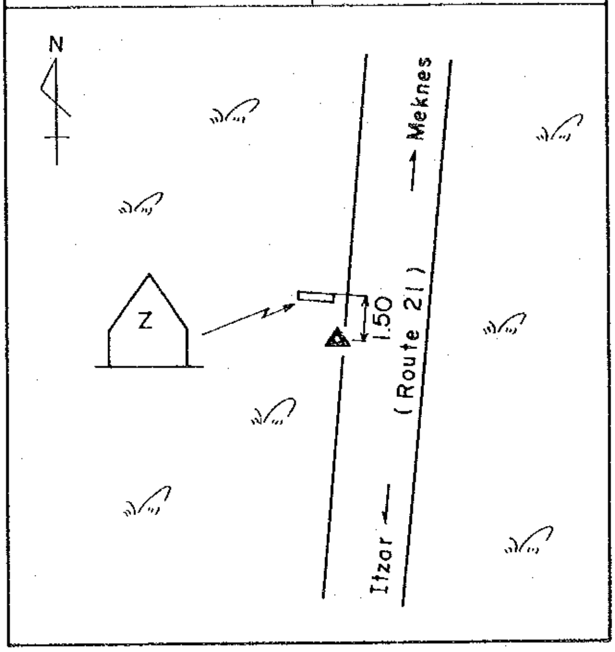

Station No.	2000	X = 541 060 m
		Y = 247 040 m
g = 979,155.410 mgal		Z = 1455.3 m (Altitude)

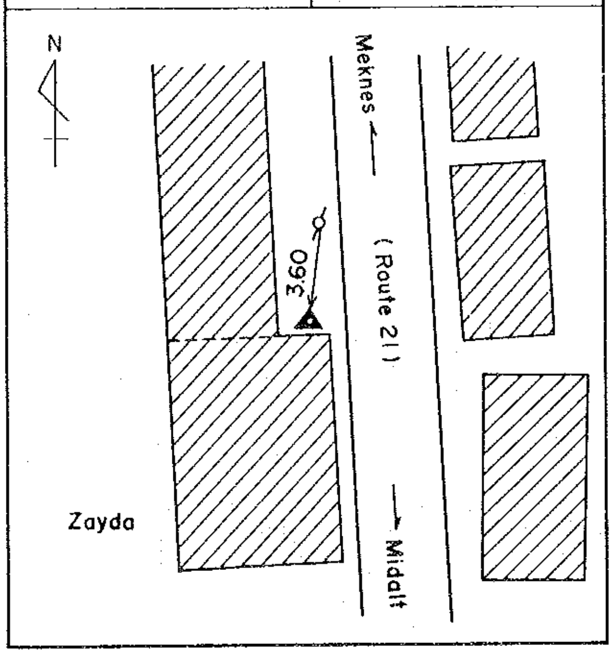

Station No.	3000	X = 541 360 m
		Y = 246 410 m
g = 979,152.892 mgal		Z = 1461.5 m (Altitude)

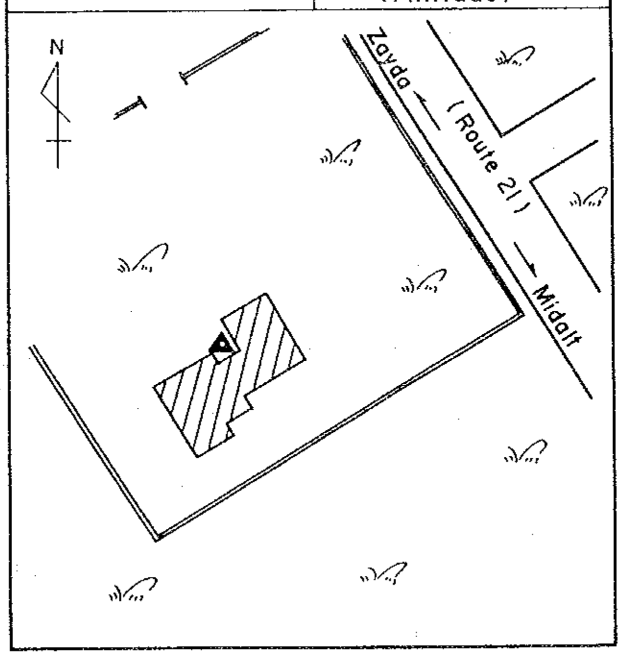

Fig. II-3 Sketches of Gravity Base Stations

Station No.	2001	X = 540 200 m
		Y = 254 520 m
g = 979,150.300 mgal		Z = 1522.65 m (Altitude)

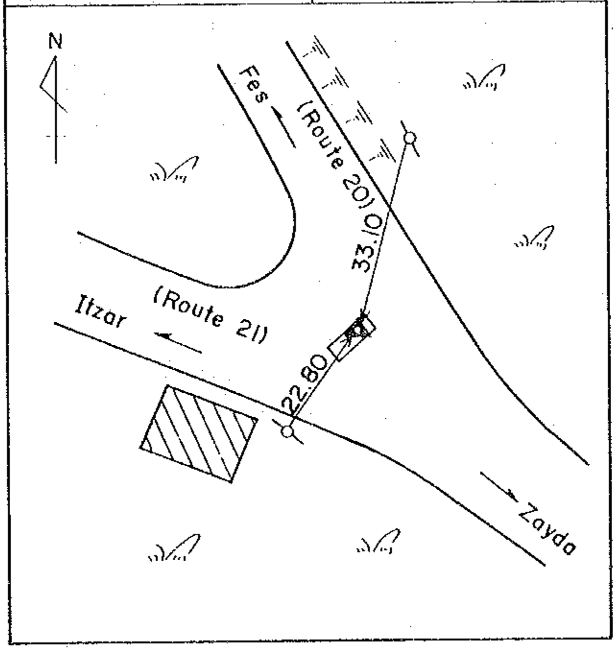

Station No.	2002	X = 528 130 m
		Y = 240 190 m
g = 979,111.124 mgal		Z = 1608.67 m (Altitude)

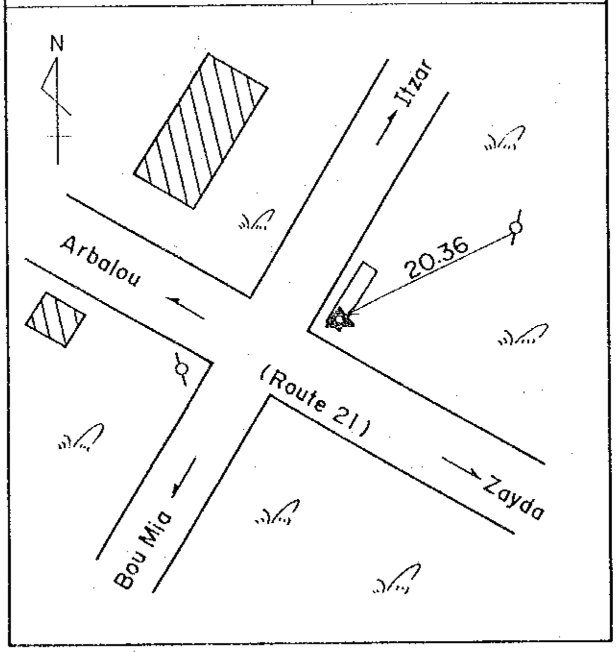

Station No.	2003	X = 538 790 m
		Y = 226 830 m
g = 979,112.782 mgal		Z = 1558.13 m (Altitude)

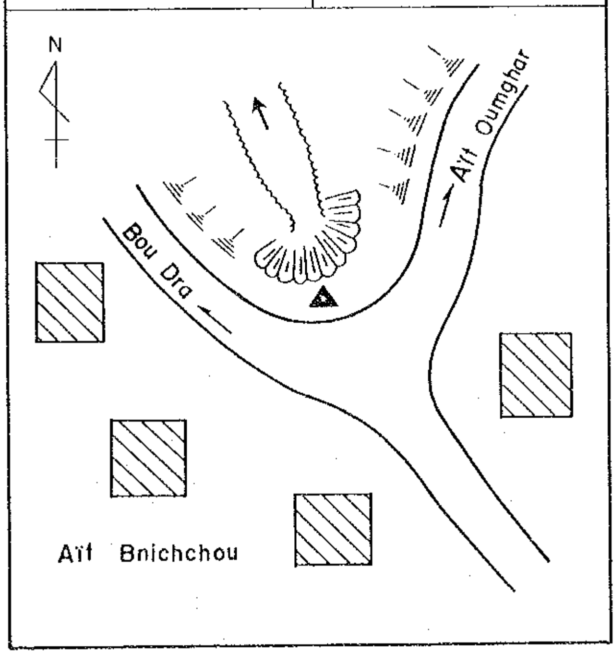

Station No.	2004	X = 549 320 m
		Y = 234 990 m
g = 979,127.233 mgal		Z = 1542.95 m (Altitude)

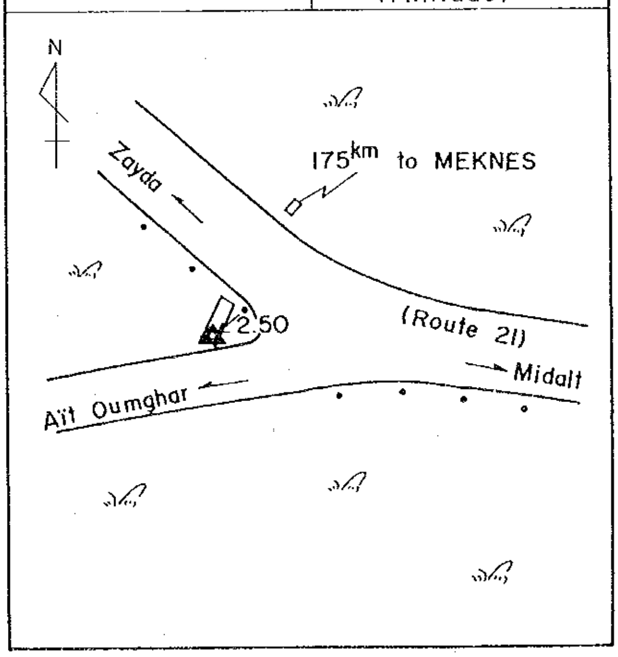

Fig. II-4 Sketches of Sub-Base Stations

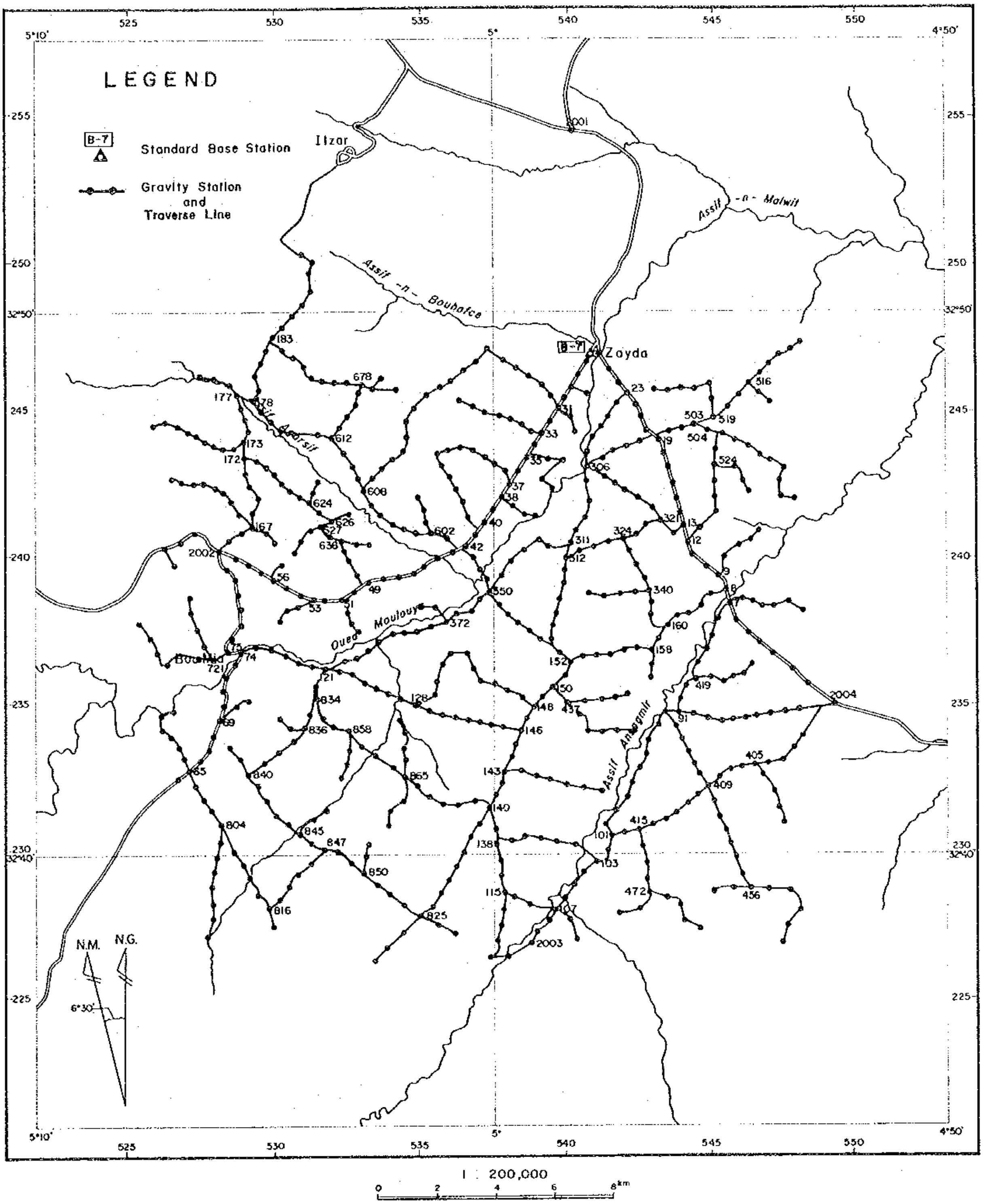

1 : 200,000

Fig. II-5 Network of Leveling Survey

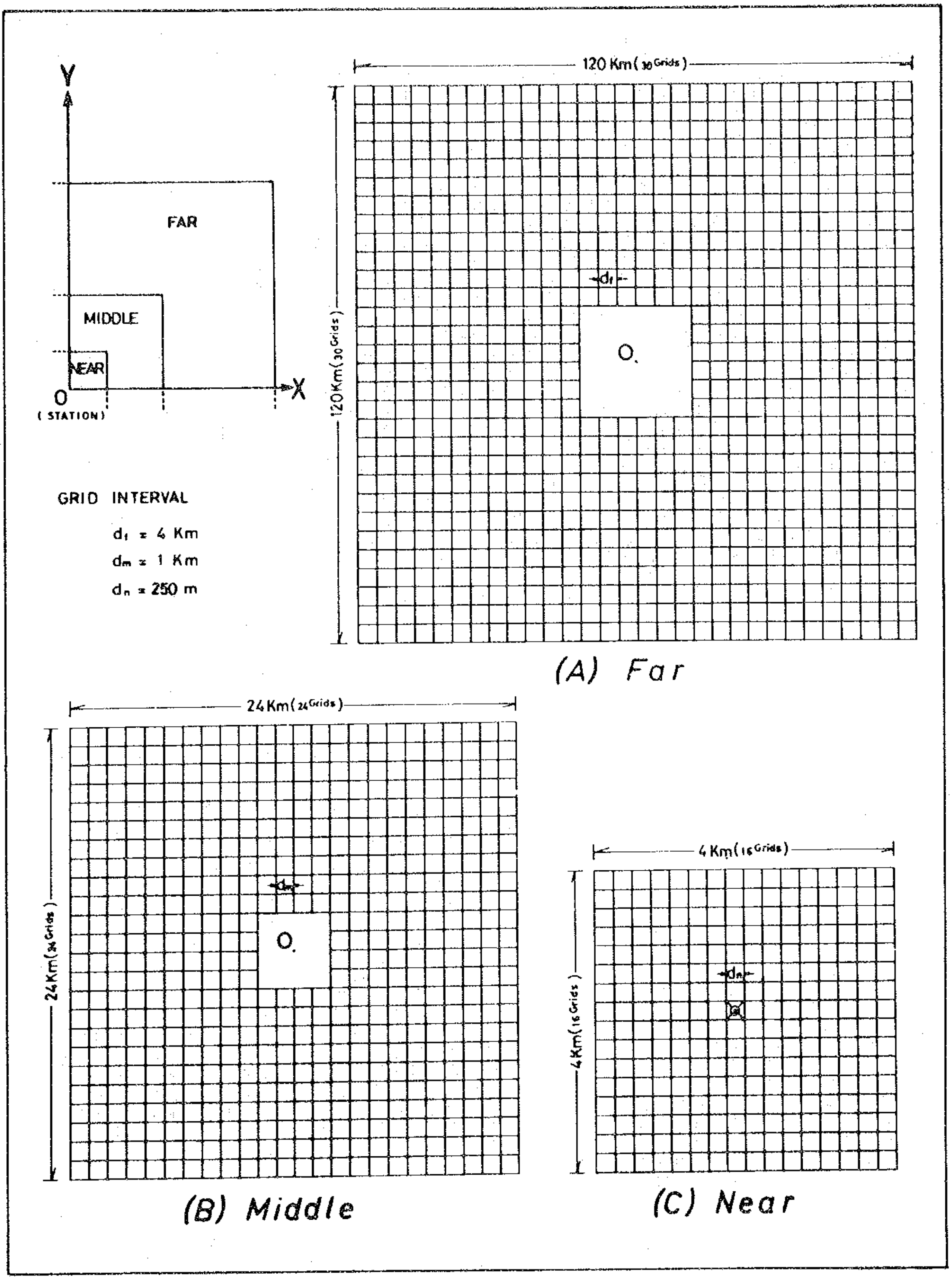

Fig. II-6 Grids of Topographical Correction

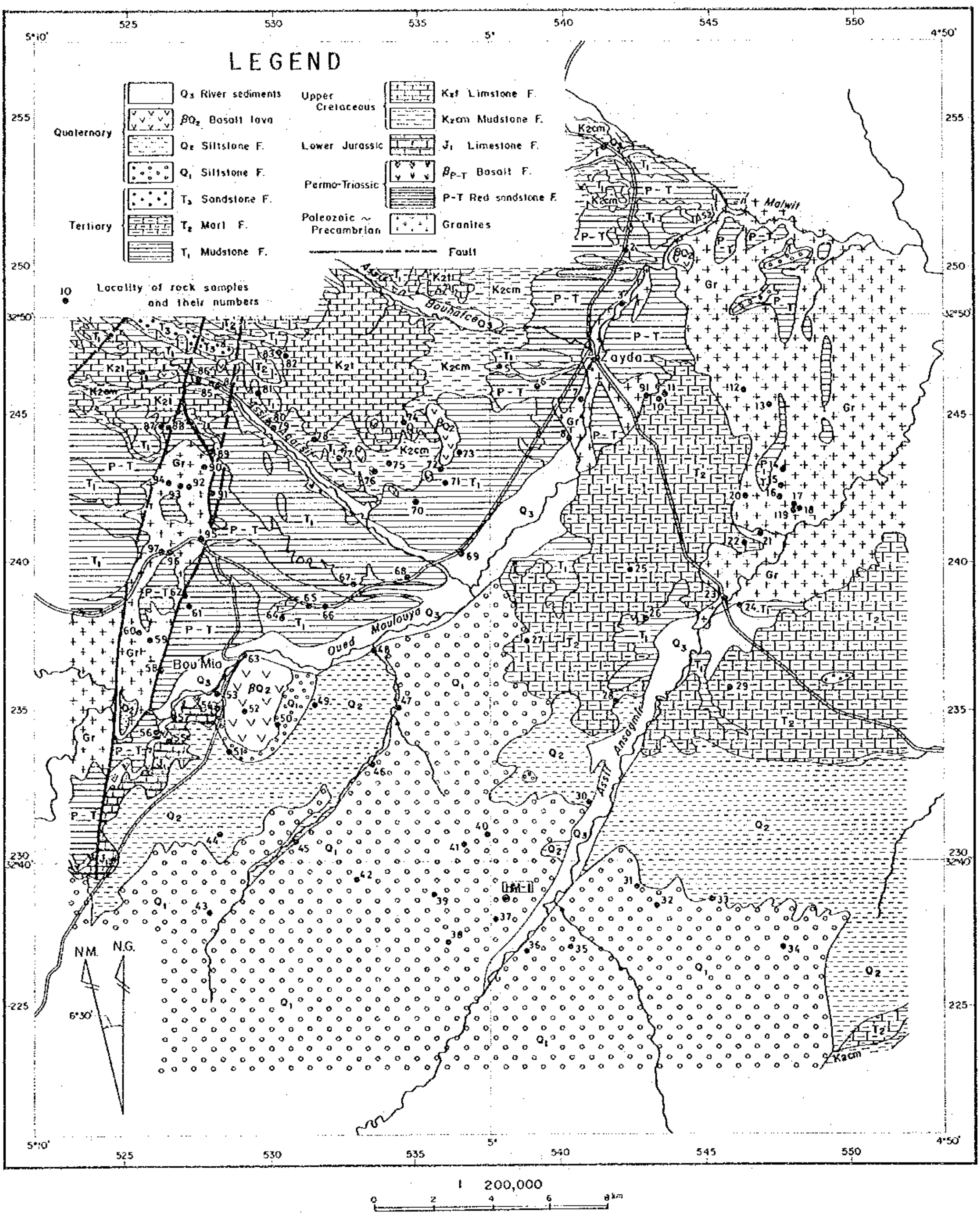

Fig. II-7 Geological Map and Locality of Rock Samples

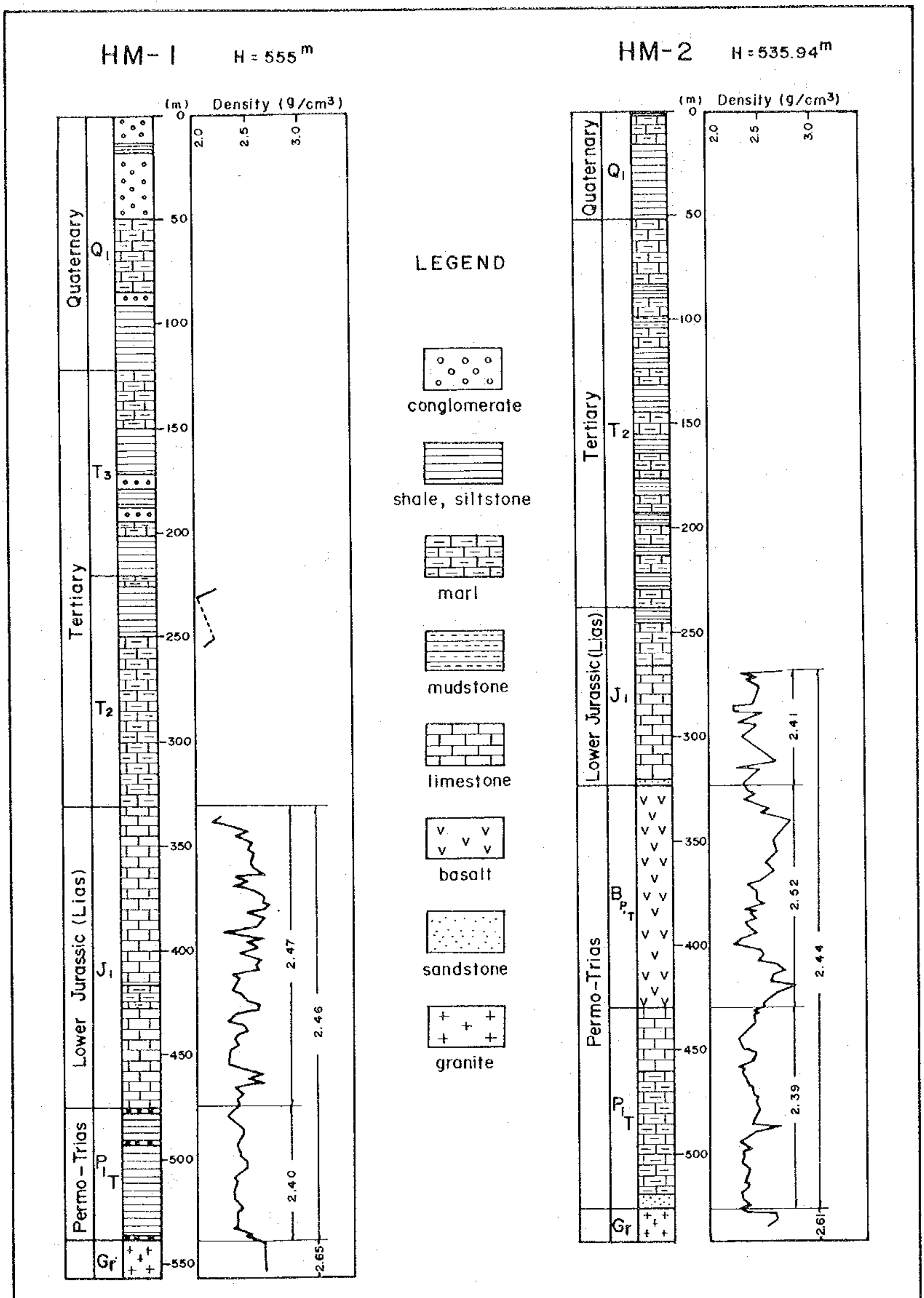

Fig. II-8 Result of Density Measurement of Boring Core

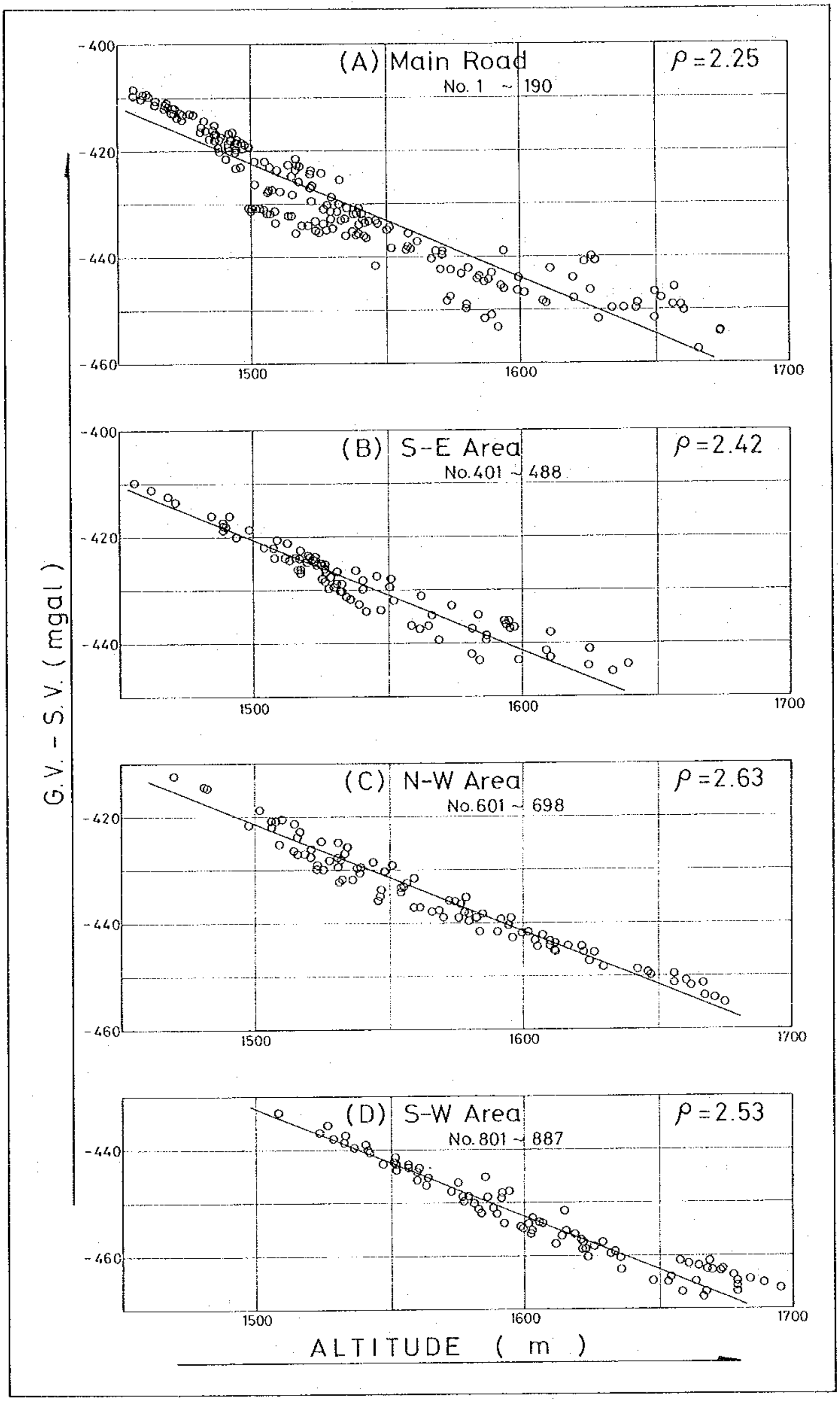

Fig. II-9 Gravimetric Value - Elevation Curve

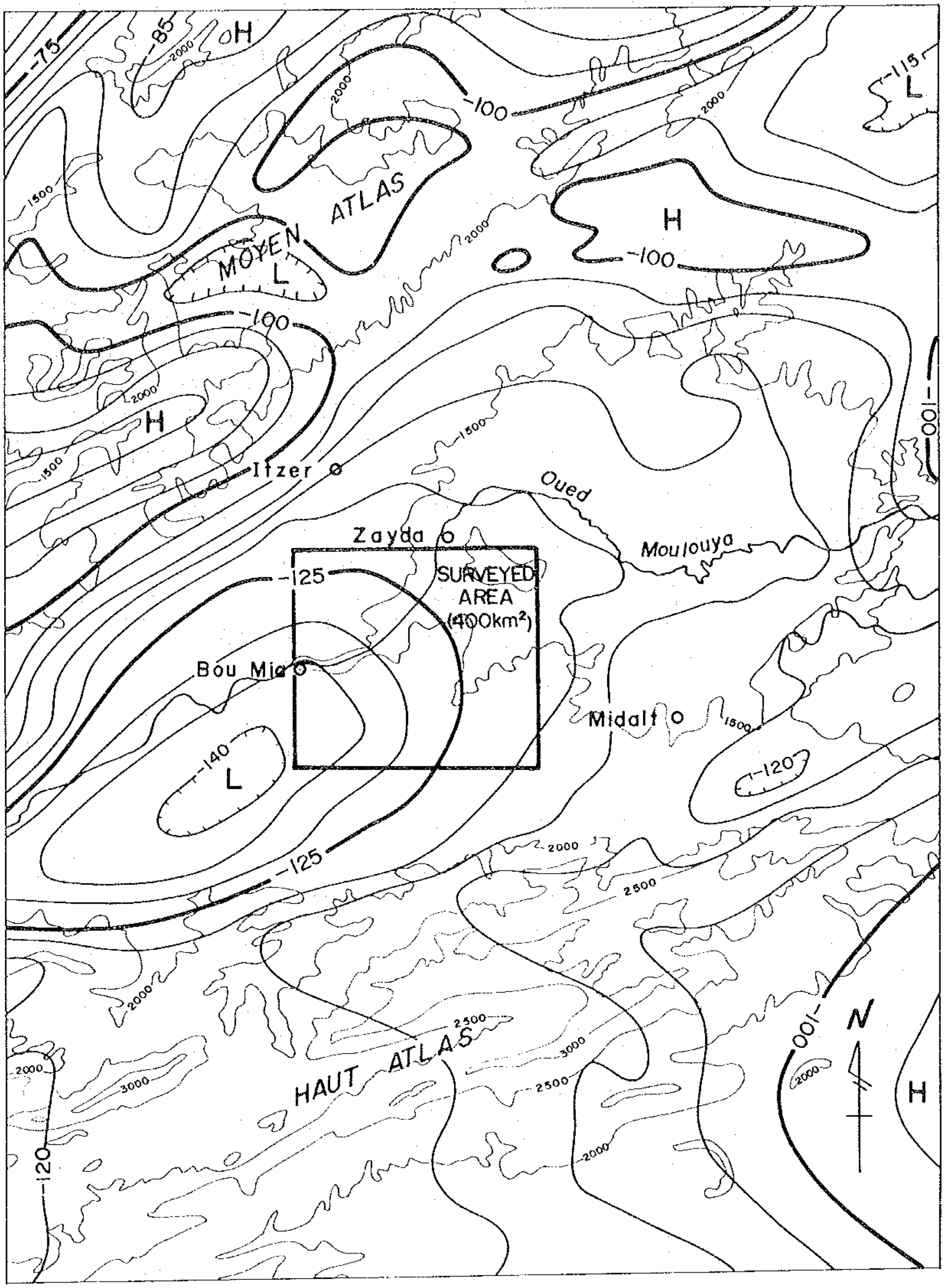

1 : 500,000
0 5 10 15 20km

Fig. II -10 Bouguer Anomaly Map on Haute Moulouya Area (ρ = 2.67)

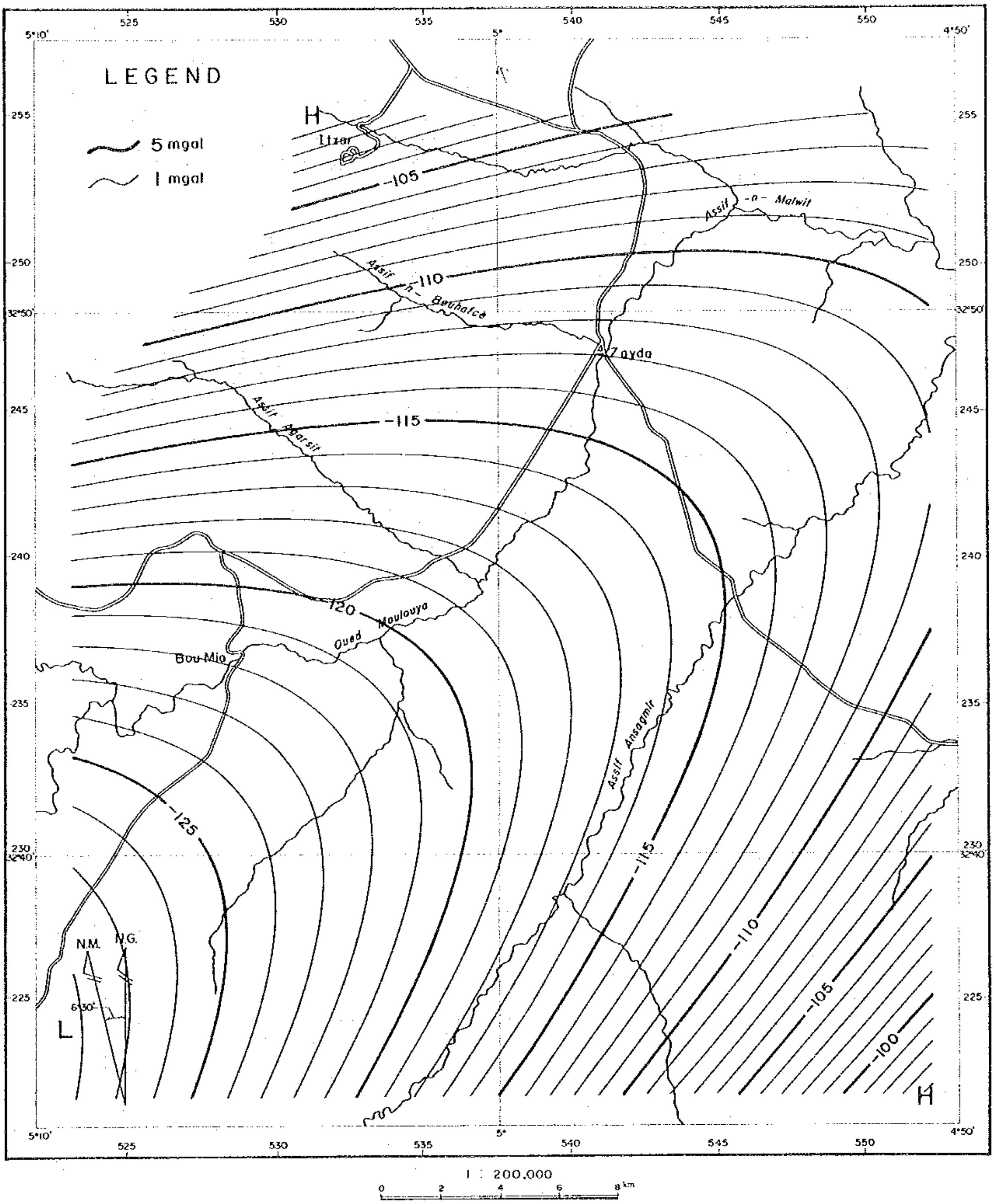

Fig. II-11 Regional Gravity Trend in Polynomial of Second Order

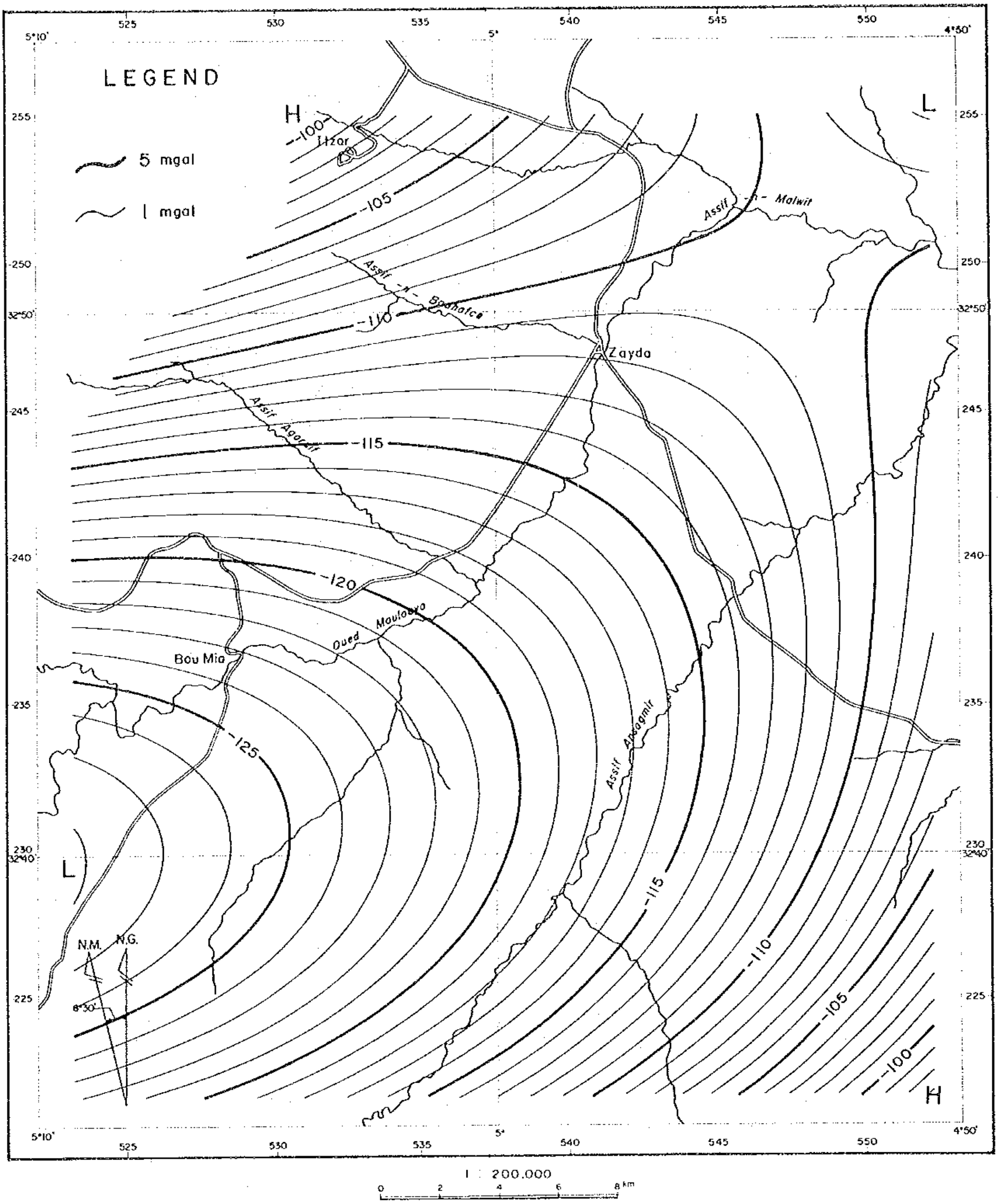

Fig. II - 12 Regional Gravity Trend in Polynomial of Third Order

Table II—2 Cretaceous Molluscan Fossils of the District

Campanian	Early	Pen	Upper	Delawarella danei Placenticeras meeki
Santanian	Late ~ Middle		Lower	Inoceramus (Platyceramus) cf. platinus
	Middle ~ Early	San Vic-ente	upper	Inoceramus (Cladoceramus) undlatoplicatus Texanites (Texanites) cf. Texanus
	Early			Inoceramus (Platyceramus) ex gr. cycloides
Coniacian	Late ~ Middle		middle	Inoceramus cf. subquadrates Inoceramus cf. stantoni
	Early		lower	Didymotis sp.
Turonian	Late	Boqui-llas	upper	Inoceramus aff. perplexus Inoceramus (Mytiloides) aff. latus
	Middle		middle	Inoceramus (Inoceramus) ex gr. lamarrki
	Early		lower	Inoceramus (Mytiloides) labiatus
Cenomanian	Middle Early	Buda		Inoceramus aff. crippsi
	Early	Del Rio		Budaiceras sp.
Albian	Late	Santa Elena		
	Middle	Sue Peaks	upper	Oxytropidoceros (Adkinsites) bravoensis
			middl	Hoplites sp.
			lower	Cleoniceras sp.
	?			
	Early	Auro-ra	upper	Douvilleiceras sp.
				Hypacanthoplites sp. Acanthohoplites sp.
Aptian	Late	La Peña		Australiceras sp.

(This list is prepared by the leading fossils collected by the regional and semi-detailed survey.)

Table II—3 Calculation of gravity values at base stations

No. of Gravity Meter & Date	No. of Station	Time	Reading Value	x Factor	Correction of Tidal Gravity (mgal)	Height of Gravity Meter (m)	Correction of Instrument Height (mgal)	Corrected Value (mgal)	Correction of Diural Drift (mgal)	Corrected Value (mgal)	Difference from Standard Base Station (mgal)	Standard Value (mgal)
	B-7	13:52	2701.27	2856.304	0.039	0.29	0.089	2856.432	0.000	2856.432		979,154.650
G-366	2000	13:57	2701.98	2857.055	0.040	0.29	0.089	2857.184	0.005	2857.189	0.757	979,155.407
Sep. 20 1978	B-7	14:03	2701.26	2856.293	0.040	0.29	0.089	2856.422	0.010	2856.432		
	2000	14:08	2701.98	2857.055	0.041	0.29	0.089	2857.185	0.009	2857.194	0.762	979,155.412
	B-7	14:13	2701.26	2856.293	0.041	0.29	0.089	2856.423	0.009	2856.432		
	B-7	11:26	2698.72	2853.612	0.021	0.29	0.089	2853.722	0.000	2853.722		979,154.650
G-366	3000	11:33	2697.06	2851.856	0.025	0.29	0.089	2851.970	-0.004	2851.966	-1.756	979,152.894
Oct. 4 1978	B-7	11:39	2698.72	2853.612	0.028	0.29	0.089	2853.729	-0.007	2853.722		
	3000	11:45	2697.05	2851.845	0.031	0.29	0.089	2851.965	-0.004	2851.961	-1.761	979,152.889
	B-7	11:51	2698.71	2853.601	0.034	0.29	0.089	2853.724	-0.002	2853.722		
G-366	B-7	12:56	2698.55	2853.432	0.000	0.29	0.089	2853.521	0.000	2853.521		979,154.650
Oct. 6 1978	B-8	13:47	2662.78	2815.589	0.011	0.27	0.083	2815.683	0.004	2815.687	-37.834	979,116.816 (979,116.730)
	B-7	14:22	2698.53	2853.411	0.014	0.29	0.089	2853.514	0.007	2853.521		

Table II—4 Densities of rock samples

Sample No.	Density (g/cm^3)	Rock Name	Geological Unit	Sample No.	Density (g/cm^3)	Rock Name	Geological Unit
1	2.53	Calcareous Siltstone	$K_{2\alpha}$	50	2.80	Basalt	β_{Q_2}
2	2.50	Conglomerate	T_1	51	2.62	"	β_{Q_2}
3	2.35	Arkose Sandstone	P–T	52	2.69	"	β_{Q_2}
4	2.56	Aplitic Granite	Ap–Gr	53	2.40	Calcareous Conglomerate	Q_3
5	2.50	Calcareous Conglomerate	T_1	54	2.44	Limestone	J_1
6	2.55	Fine Grained Limestone	$K_{2\alpha}$	55	2.35	"	J_1
7	2.57	Medium Grained Granite	Gr	56	2.56	Basalt	β_{P-T}
8	2.56	Aplitic Granite	Ap–Gr	57	2.40	"	β_{P-T}
9	2.52	Arkose Sandstone	P–T	58	2.66	Barite Vein	–
10	2.54	Fine Grained Sandstone	P–T	59	2.60	Aplite	Ap–Gr
11	2.52	" "	P–T	60	2.56	Aplitic Granite	Ap–Gr
12	2.55	Aplitic Granite	Ap–Gr	61	2.49	Sandstone	P–T
13	2.63	Granite	Gr	62	2.45	"	P–T
14	2.53	Fine Grained Sandstone	P–T	63	2.72	Basalt	β_{Q_2}
15	2.56	Quartz Vein	–	64	2.33	Conglomerate	T_2
16	2.57	Granite	Gr	65	1.98	Calcareous Sandstone	T_1
17	2.64	Medium Grained Granite	Cnt–Gr	66	2.66	Limestone	T_2
18	2.57	" "	Cnt–Gr	67	2.16	Calcareous Siltstone	T_1
19	2.76	Schist	Sch	68	2.40	Calcareous Conglomerate	T_1
20	2.61	Coarse Grained Granite	Gr	69	2.50	" "	Q_3
21	2.67	Granite	Gr	70	2.45	Basalt	β_{Q_2}
22	2.63	Aplitic Granite	Ap–Gr	71	2.23	Calcareous Sandstone	T_1
23	2.66	Granite	Cnt–Gr	72	2.89	Basalt	β_{Q_2}
24	2.64	Medium Grained Granite	Cnt–Gr	73	3.05	"	β_{Q_2}
25	2.26	Limestone	T_2	74	2.56	Silty Limestone	$K_{2\alpha}$
26	2.33	"	T_2	75	2.54	" "	$K_{2\alpha}$
27	2.34	Conglomerate	T_2	76	2.98	Basalt	β_{Q_2}
28	2.44	"	Q_2	77	2.43	Calcareous Conglomerate	T_1
29	2.25	Limestone	T_2	78	2.37	Fine Grained Sandstone	T_1
30	2.38	Conglomerate	Q_2	79	2.35	Argilous Limestone	K_{2t}
31	2.33	Calcareous Mudstone	Q_1	80	2.41	" "	K_{2t}
32	2.37	Calcareous Conglomerate	Q_1	81	2.60	Limestone	K_{2t}
33	2.17	Calcareous Siltstone	Q_2	82	2.46	"	T_1
34	2.50	Conglomerate	Q_1	83	2.61	"	T_1
35	2.16	Calcareous Conglomerate	Q_1	84	2.30	Calcareous Siltstone	K_{2t}
36	2.41	Conglomerate	Q_1	85	2.60	Limestone	$K_{2\alpha}$
37	2.44	"	Q_1	86	2.49	"	K_{2t}
38	2.38	Calcareous Silty Sandstone	Q_1	87	2.44	"	$K_{2\alpha}$
39	2.39	Limestone	Q_1	88	2.52	"	$K_{2\alpha}$
40	2.36	Calcareous Conglomerate	Q_1	89	2.59	Aplitic Granite	Ap–Gr
41	2.34	Limestone	Q_1	90	2.47	Arkose Sandstone	P–T
42	1.81	Calcareous Siltstone	Q_1	91	2.64	Granite	Gr
43	2.29	Calcareous Conglomerate	Q_1	92	2.69	"	Gr
44	1.87	Calcareous Siltstone	Q_2	93	2.63	Aplitic Granite	Ap–Gr
45	2.51	Conglomerate	Q_2	94	2.59	Granite	Gr
46	2.49	"	Q_1	95	2.58	Aplitic Granite	Ap–Gr
47	2.26	Medium Grained Sandstone	Q_2	96	2.59	Medium Grained Granite	Gr
48	2.55	Quartz Vein	–	97	2.56	Aplite	Ap–Gr
49	2.56	Conglomerate	Q_2				

LEGEND

Quaternary { Q_3, β_{Q_2}, Q_2, Q_1 }

Tertiary { T_2, T_1 }

Upper Cretaceous { K_{2t}, $K_{2\alpha}$ }

Lower Jurassic J_1

Permo-Triassic { β_{P-T}, P–T }

Paleozoic ~ Precambrian { Ap–Gr, Gr, Cnt–Gr, Sch }

Table II—5 Distribution of rock densities

Geological Age		Geological Unit and Mark		Lithology	Amount	Average of Density		Density (g/cm^3) 2.0 2.5 3.0
Cenozoic	Quaternary		Q_3	terrace deposit	2	2.45	2.33	
			Q_2	conglomerate, siltstone, mudstone	7	2.31		
			Q_1	conglomerate, siltstone	13	2.33		
			β_{Q2}	basalt lava	8		2.78	
	Tertiary		T_2	marl, limestone, siltstone, conglomerate	6	2.36	2.36	
			T_1	light brown siltstone, conglomeratic sandstone	10	2.36		
Mesozoic	Upper Cretaceous	Turonian	K_{2t}	micritic limestone, muddy siltstone, calcareous siltstone, turbidite	5	2.43	2.49	
		Cenomanian	K_{2cm}	limestone, calcareous siltstone, poly-colored siltstone, gypsum bed	7	2.53		
	Lower Jurassic	Lias	J_1	limestone, siltstone, marl, sandstone, conglomerate, turbidite, dolomite	2		2.40	
	Permo-Triassic	Permo-Trias	β_{P-T}	basalt lava, sandstone, conglomerate	2	2.48	2.48	
			P-T	red sandstone, arkose sandstone, siltstone, mudstone	8	2.48		
Proterozoic ~ Paleozoic	Paleozoic ~ Precambrian	Basement Complex	Ap-Gr	aplitic granite	10	2.58	2.60	
			Gr	granite	9	2.62		
			Cnt-Gr	contaminated granite	4	2.63		
Others				quartz vein, barite vein, schist	4	–	–	

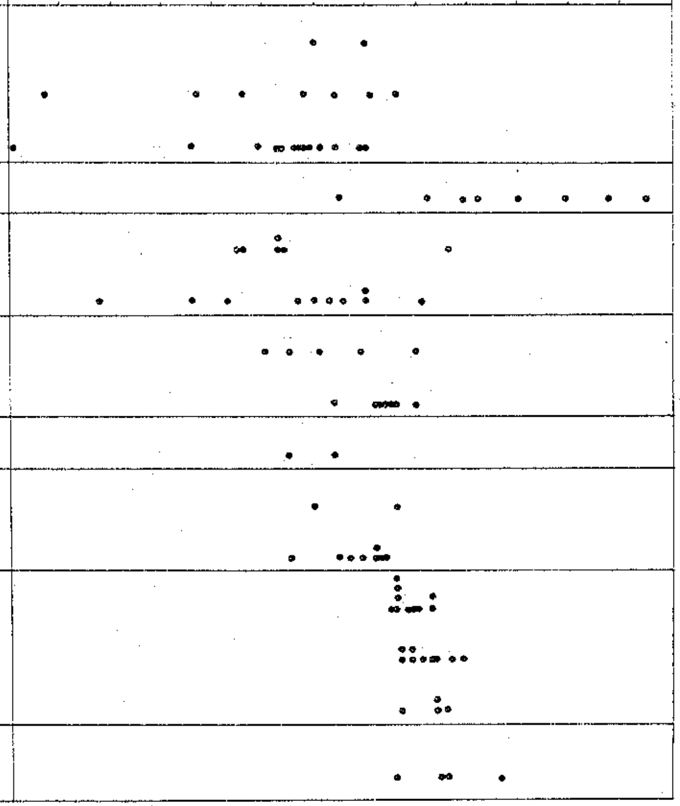

APPENDICES

(Geological Survey)

(Geophysical Survey)

Table I—2 List of Rock Samples

(1)

Sample No.		Location			Rock Name	Dating ○ XMA △ X-ray ▲	Chemical Analysis of Rock					T.S.	P.S.
		X	Y	Z			W.C.	M.C.	U.T.V.	U.T.	Met.		
1	1A02	545.0	251.7	1435	Porphyritic gr					○			
2	1A07	547.2	251.2	1415	Fe-qz vein					○			
3	1A11	540.2	245.8	1470	Aplitic gr	○	○			○		○	
4	1A12	540.7	242.9	1480	Pb-ore						○		○ 13
5	1A14	542.6	248.9	1450	Limonitized sheared gr-porphyry					○			
6	1B04	548.7	248.7	1435	Contaminated gr	○	○			○		○ 1	
7	1B05	548.7	249.7	1430	Aplitic gr			○		○		○ 2	
8	1B09	551.5	250.6	1430	Gr-porphyry					○		○	
9	1C02	546.0	238.9	1450	Contaminated gr			○		○			
10	1C12	546.4	242.0	1490	Aplitic gr			○		○			
11	1D01	551.6	252.1	1400	Arkose ss						○		
12	1D05	546.1	251.9	1380	Arkose ss				○				
13	1D10	549.6	250.8	1430	Gr-porphyry					○			
14	1D13	548.2	251.3	1400	Gr-porphyry	△				○			○
15	1D14	551.4	251.3	1390	Arkose ss				○				
16	1D15	551.3	251.1	1410	Arkose ss	△			○			○ 3	○ 17
17	1D16	550.0	251.3	1410	Gr-porphyry					○			
18	1D18	542.8	251.3	1450	Red siltstone				○				
19	1D19	543.4	250.4	1430	Galena-arkose ss						○		
20	1D20	548.0	251.5	1400	Porphyritic gr			○		○		○ 4	

W.C.: Whole Composition
M.C.: Main Composition
U.T.V.: analysis for Uranium, Thorium, Vanadium
U.T.: analysis for Uranium, Thorium
Met.: Metal Composition (Pb, Cu, Ba, Au, Ag)
T.S.: Thin Section
P.S.: Polished Section
gr: granite
ss: sandstone
Qz: quartz
○ 13: Number of Photomicrograph

(2)

Sample No.		Location			Rock Name	Dating ○ XMA △ X-ray ▲	Chemical Analysis of Rock					T.S.	P.S.
		X	Y	Z			W.C.	M.C.	U.T.V.	U.T.	Met.		
21	1E01	554.3	244.1	1500	Pb-ore						○		
22	1E07	551.2	240.9	1500	do						○		○14
23	1E08	554.4	241.6	1460	do						○		
24	1E09	554.4	241.6	1460	do						○		
25	1E10	553.5	241.4	1495	do						○		
26	1E11	552.2	241.0	1500	do						○		○
27	1E12	552.2	241.0	1500	do						○		
28	1E14	553.8	247.0	1430	do						○		
29	1F05	558.7	244.0	1300	Pb-fluorite vein						○		
30	1F11	556.1	244.0	1390	Calcareous siltstone				○				
31	1F12	556.1	244.0	1390	Muddy siltstone				○				
32	1F13	556.1	244.0	1390	do				○				
33	1F14	556.0	242.7	1400	Barite vein						○		
34	1G12	555.2	249.0	1465	Fe-qz vein					○			
35	1G15	554.3	250.0	1450	Fe-qz vein					○			
36	1G19	557.6	251.6	1430	Fe-qz vein					○			
37	1J18	565.3	251.0	1405	Granite			○		○			
38	1K08	571.5	253.7	1320	Fe-qz vein	△				○			○
39	1K09	571.4	253.5	1320	Granodiorite			○		○		○ 5	
40	1K22	571.8	253.1	1340	Microgranodiorite					○		○ 6	
41	1K31	567.4	255.4	1345	Pb-ore						○		○15
42	1K32	569.8	255.3	1330	do						○		
43	2A04	524.9	235.4	1550	Aplitic gr			○		○		○	
44	2A07	527.9	243.5	1600	Arkose ss						○		
45	2A08	527.9	243.5	1600	do						○		

Sample No.		Location			Rock Name	Dating ○ XMA △ X-ray ▲	Chemical Analysis of Rock					T.S.	P.S.
		X	Y	Z			W.C.	M.C.	U.T.V.	U.T.	Met.		
46	2A09	527.9	243.5	1600	Arkose ss						○		
47	2A10	527.9	243.5	1600	do						○		
48	2A11	527.9	243.5	1600	do						○		
49	2A12	527.9	243.5	1600	do						○		
50	2A13	527.9	243.5	1600	Aplitic gr(carapace)	△			○			○ 7	○ 18
51	2A24	525.3	241.7	1660	Arkose ss						○		
52	2A25	525.3	241.7	1660	do						○		
53	2B06	521.5	231.3	1675	Pb-Ba ore						○		
54	2B07	521.3	231.2	1780	do						○		
55	2B20	520.7	236.6	1675	Arkose ss						○		
56	2B21	521.3	235.5	1685	do						○		
57	2B23	521.6	234.7	1700	do			○					
58	2B24	521.7	234.6	1700	Aplitic gr			○		○			
59	2B25	520.4	234.8	1650	do						○		
60	2B26	520.0	232.9	1620	Arkose ss						○		
61	2B28	520.6	233.6	1680	Aplite		○			○		○ 8	
62	2B29	523.3	234.3	1600	Porphyritic gr	○	○			○		○	
63	2B30	525.6	235.5	1560	Gr-porphyry		○			○		○ 9	
64	2B31	525.6	235.5	1560	do			○		○		○	
65	3R05	516.3	255.0	1780	Arkose ss					○			
66	3R06	516.3	255.0	1780	do					○			
67	3R08	516.3	255.0	1780	do					○			
68	3R09	516.3	255.0	1780	do					○			
69	3R11	517.5	253.7	1980	do					○			
70	3R12	517.5	253.7	1980	do					○			

Sample No.		Location			Rock Name	Dating ○ XMA △ X-ray ▲	Chemical Analysis of Rock					T.S.	P.S.
		X	Y	Z			W.C.	M.C.	U.T.V.	U.T.	Met.		
71	3R13	517.5	253.7	1980	Arkose ss					○			
72	3R14	517.5	253.7	1980	do					○			
73	3R15	517.5	253.7	1980	do					○			
74	4I04	562.7	238.6	1440	Pb-ore						○		○
75	4I05	562.7	238.6	1440	do						○		○
76	4I06	562.7	238.5	1450	do						○		
77	4J14	570.6	240.6	1385	do						○		○16
78	4J15	570.6	240.6	1385	do						○		○
79	4J16	570.6	240.6	1385	do						○		
80	4J17	569.9	240.2	1400	do						○		
81	M001	539.7	244.7	1510	Mineralized arkose ss							○10	○
82	M002	548.2	251.4	1410	Granite							○11	
83	M003	517.6	241.3	1650	do							○	
84	M004	517.6	241.3	1650	Arkose ss							○	
85	M005	517.6	241.3	1650	Fine-grained ss							○12	
86	M006	547.7	251.5	1400	Granite							○	
87	M007	547.8	251.5	1400	Contaminated gr							○	
88	M008	517.6	241.3	1650	Decolorized siltstone	▲							
89	M009	517.6	241.3	1650	Red siltstone	▲							

Table I—3 Chemical Analysis of Granitic Rocks

Sample No	1 (1A11)	2 (1B04)	3 (2B28)	4 (2B29)	5 (2B30)
Rock Name	Aplitic granite	Contaminated granite	Aplite	Porphyritic granite	Granite porphyry
Chemical Composition	wt (%)	wt (%)	wt (%)	wt (%)	wt (%)
SiO_2	77.88	73.97	77.60	71.85	78.22
TiO_2	0.093	0.34	0.057	0.39	0.26
Al_2O_3	12.48	13.87	12.81	14.92	12.59
Fe_2O_3	0.56	0.80	0.87	0.92	1.09
FeO	0.43	0.94	0.20	1.64	0.37
MnO	0.026	0.032	0.005	0.087	0.004
MgO	0.10	0.17	0.10	0.64	0.07
CaO	0.45	1.19	0.31	1.30	0.13
Na_2O	2.13	1.91	2.26	2.75	0.89
K_2O	4.54	4.44	4.43	3.79	5.18
P_2O_5	0.01	0.11	0.02	0.13	0.079
H_2O+	0.13	0.51	0.14	0.53	0.06
H_2O-	0.33	0.76	0.31	0.45	0.40
Total	99.159	99.042	99.112	99.397	99.343

Sample No	6 (1B05)	7 (1C02)	8 (1C12)	9 (1D20)	10 (1J18)
Rock Name	Aplitic granite	Contaminated granite	Aplitic granite	Porphyritic granite	Granite
Chemical Composition	wt (%)	wt (%)	wt (%)	wt (%)	wt (%)
SiO_2	75.87	64.88	75.64	71.54	72.01
Al_2O_3	11.78	14.82	12.36	12.53	14.20
CaO	0.68	1.85	0.56	1.04	1.31
Na_2O	3.82	3.23	2.79	2.66	3.57
K_2O	3.45	4.10	4.41	4.62	3.40
Total	95.60	88.88	95.76	92.39	94.49

Sample No	11 (1K09)	12 (2A04)	13 (2B23)	14 (2B24)	15 (2B31)
Rock Name	Granodiorite	Aplitic granite	Arkose sandstone	Aplitic granite	Granite porphyry
Chemical Composition	wt (%)	wt (%)	wt (%)	wt (%)	wt (%)
SiO_2	54.96	77.22	75.34	75.30	75.89
Al_2O_3	15.67	11.29	12.63	12.63	12.10
CaO	5.05	0.46	0.40	0.43	0.15
Na_2O	2.26	3.07	3.10	3.31	1.59
K_2O	3.33	4.55	4.50	4.14	4.79
Total	81.27	96.59	95.97	95.81	94.52

Table I—4 C.I.P.W. Norm Calculation

Sample No / Rock Name / Normative Minerals	1. (1A11)		2. (1B04)		3. (2B28)		4. (2B29)		5. (2B30)	
	Aplitic granite		Contaminated granite		Aplite		Porphyritic granite		Granite porphyry	
	wt.(%)	mol.(%)	wt.(%)	mol.(%)	wt.(%)	mol.(%)	wt.(%)	mol.(%)	wt.(%)	mol.(%)
Q	47.54	85.60	44.11	82.28	47.38	85.27	37.77	76.77	53.67	86.67
C	3.31	3.51	4.11	4.52	3.83	4.06	4.31	5.16	5.54	5.27
Or	27.18	5.28	26.83	5.40	26.53	5.15	22.76	4.99	30.96	5.40
Ab	18.26	3.77	16.53	3.53	19.38	4.00	23.64	5.51	7.62	1.41
An	2.20	0.85	5.30	2.14	1.43	0.55	5.69	2.50	0.12	0.04
Salic total	98.49	99.02	96.89	97.88	98.55	99.03	94.16	94.93	97.90	98.79
En-Hy	0.25	0.27	0.43	0.48	0.25	0.27	1.62	1.97	0.18	0.17
Fs-Hy	0.24	0.19	0.57	0.49	–	–	1.80	1.67	–	–
Mt	0.82	0.38	1.19	0.57	0.51	0.24	1.36	0.71	0.44	0.19
Hm	–	–	–	–	0.53	0.36	–	–	0.80	0.48
Il	0.17	0.12	0.66	0.49	0.12	0.08	0.75	0.61	0.50	0.32
Ap	0.02	0.01	0.26	0.09	0.05	0.02	0.31	0.11	0.19	0.06
Femic total	1.51	0.98	3.11	2.12	1.45	0.97	5.84	5.07	2.10	1.21
Q+Or+Ab+An	95.18		92.77		94.72		89.86		92.37	
Q	49.95		47.55		50.02		42.03		58.10	
Or+Ab	47.74		46.74		48.47		51.64		41.77	
An	2.31		5.71		1.51		6.33		0.13	

Table I—5 K-Ar Age Determination of Granitic Rocks

Sample No.	Rock Name	Location	Mineral	$Ar^{40}R/K^{40}$	Age (m.y.)	Argon Analysis			Potassium Analysis		
						$Ar^{40}R$, ppm	$Ar^{40}R$/Total Ar^{40}	Ave. Ar^{40}, ppm	K, %	Ave. K, %	K^{40}, ppm
1A11	Aplitic granite	Zayda	Biotite	0.01904	300 ± 11	0.1625 0.1620	0.853 0.891	0.1623	7.135 6.837	6.986	8.522
1B04	Contaminated granite	Tighbouba -n-Ouzour	Biotite	0.01954	307 ± 11	0.1402 0.1447	0.929 0.887	0.1425	5.794 6.159	5.976	7.291
2B29	Porphyritic granite	Bou Mia	Biotite	0.01943	306 ± 11	0.1552 0.1595	0.942 0.821	0.1574	6.618 6.656	6.637	8.097

Constants Used

$\lambda\beta = 4.72 \times 10^{-10}$ /year

$\lambda e = 0.585 \times 10^{-10}$ /year

$K^{40}/K = 1.22 \times 10^{-4}$ g./g.

$$Age = \frac{1}{\lambda e + \lambda\beta} \ln\left[\frac{\lambda\beta + \lambda e}{\lambda e} \times \frac{Ar^{40}R}{K^{40}} + 1\right]$$

Note: $Ar^{40}R$ refers to radiogenic Ar^{40}.

m.y. refers to millions of years.

Table I—6 Microscopic Observations

(1)

Sample No.	Location	Formation	Rock Name	Microscopic Observation	Remark
1A11	Zayda	Basement Granites	Aplitic Granite	This is granular in texture and mainly composed of quartz, plagioclase, orthoclase and biotite. Anhedral quartz shows weak wavy extinction and up to 2.0 mm in size. Anhedral plagioclase (oligoclase) shows albite twinning and weak zonal structure, core part of which is suffered of weak sericitization. Plagioclase is about 1.0 mm in length. Anhedral orthoclase shows Carlsbad twinning and perthite structure, up to 2.0 mm in length. In part, orthoclase shows mirmekite texture with quartz and plagioclase. Subhedral biotite is light to dark brown and about 1.0 mm in length. Some parts are affected by chloritization and iron-oxidization. Other accessary minerals are fine grained zircon, apatite and opaque minerals.	
1B04	Tighbouba-n-Ouzour	Basement Granites	Contaminated Granite	The rock shows granular texture and is mainly composed of quartz, plagioclase, orthoclase and biotite. Quartz is anhedral in form and up to 4.0 mm in size. It shows wavy extinction. Plagioclase shows subhedral and albite twinning, up to 3.0 mm in length. Plagioclase is more calcic than the above menthoned sample and shows zonal structure, core part of which is affected by sericitization. Anhedral orthoclase shows carlsbad twinning and perthite structure. Some orthoclases have included of small grained(up to 0.5 mm) plagioclase, quartz and biotite crystals. This means orthoclase is final crystallized mineral. Biotite is above 1.0 mm is size and light - dark brown in colour. Other accessary minerals are zircon, apatite and opaque minerals.	Photomicrograph No. 1
1B05	Tighbouba-n-Ouzour	Basement Granites	Aplitic Granite	This texture, constituent minerals and their occurence are the same as the above mentioned rock No. 1A11	Photomicrograph No. 2

Sample No.	Location	Formation	Rock Name	Microscopic Observation	Remark
1B09	South of Paneau-1	Basement Granites	Granite Porphyry	This shows porphyritic texture by crushing. So, phenocryst is granite fragment and matrix is made of crushed granitic materials. Quartz of the fragment shows strong wavy and partial extinction. Orthoclase shows carlsbad twinning and weak perthite structure. Plagioclase shows albite twinning which is broken by crushing, those minerals of the fragment are anhedral in form and about 0.5 - 1.0 mm in size. Matrix is composed of fine grained (0.01 - 0.5 mm) anhedral quartz and feldspars. Whole parts of the matrix is affected by iron-oxidization.	
1D15	Paneau-1	P-T Red Sandstone	Arkose Sandstone	The rock shows clastic texture and composed of quartz, orthoclase, plagioclase and granite fragment. All of the fragments are rounded and about 1.0 - 2.0 mm in size. Quartz shows wavy extinction. Orthoclase shows carlsbad twinning and perthite structure. Plagioclase shows albite twinning. Granite fragment is made of quartz, orthoclase and a few amount of plagioclase. Matrix has been recrystallized and composed of fluorite, hematitie, very fine felsic minerals and opaque minerals. Fluorite is anhedral in form and colourless to blue in colour. The fluoritization has occured in feldspars fragment. Barite shows euhedral and is aggregated in lathlike form. The other matrix minerals is anhedral and occurs like sementation of the fragments.	Photomicrograph No. 3, No. 17 7,000 c/s
1D20	Assaka-n-Tabhirt	Basement Granites	Porphyritic Granite	This is granular in texture and mainly composed of orthoclase, quartz, plagioclase and biotite. Orthoclase is very large crystal, more than 20 mm in length. It shows Carlsbad twinning and perthite structure. The parts of albite composition in perthite shows albite twinning. Anhedral quartz shows wavy extinction and up to 2.0 mm in size. Subhedral phagioclase (oligoclase) shows albite twinning and zonal structure (up to 4.0 mm in length). Biotite is subhedral in form and light to dark in colour (up to 2.0 mm in length). Other accessary minerals are apatite, zircon and opaque minerals.	Photomicrograph No. 4

Sample No.	Location	Formation	Rock Name	Microscopic Observation	Remark
1K09	Sidi Ayyad	Basement Granites	Granodiorite	This is granular in texture and mainly composed of plagioclase, quartz, microcline, biotite and hornblende. Plagioclase is euhedral to subhedral in form and up to 2.0 mm in length. It shows albite twinning and zonal structure and is affected by sericitization. Quartz is anhedral in form and up to 0.5 mm in size. Microcline shows microcline-structure and anhedral form (up to 0.3 mm in size). Biotite is subhedral to anhedral in form and light to dark brown in colour (about 1.0 mm in length). Hornblende is subhedral to euhedral in form and colourless to green in colour (about 1.5 mm in length). The mafic minerals are partly affected by chloritization. Other accessary minerals are sphene, zircon, epidote, apatite and opaque minerals.	Photomicrograph No. 5
1K22	Sidi Ayyad	Basement Granites	Microgranodiorite	This is granular in texture and mainly composed of quartz, plagioclase, orthoclase and mafic minerals. This is affected by strong chloritization, sericitization and iron oxidization, and intruded by many quartz, sericite and copper veins. Quartz shows anhedral form and about 0.2 mm in size. Feldspars are suffered sericitization and iron-oxidization, so they show slightly albite and carlsbad twinning. They are subhedral to anhedral in form and up to 0.5 mm in length. Mafic minerals are perfectly altered to chlorite, which shows aggregated form accompained by opaque minerals. Vein is about 0.2 mm in width and composed of quartz, sericite malachite, cuprite and opaque minerals. Apatite occurs in needle-shaped and granular-shaped.	Photomicrograph No. 6
2A04	Bou Mia	Basement Granites	Aplitic Granite	This is granular in texture and mainly composed of quartz, orthoclase, plagioclase and biotite. Quartz shows anhedral form (up to 2.0 mm in size) and wavy extinction. Anhedral orthoclase shows carlsbad twinning and perthite structure, albite part of which has albite twinning. Orthoclase is up to 4.0 mm in length, and shows mirmekitic texture in its margin. Plagioclase is anhedral in form and about 1.0 mm in length. It shows albite twinning and weak zonal structure. Biotite is subhedral in form and redish brown to light brown in colour. It has pleochroic halo by zircon. Other accessary minerals are muscovite, apatite and opaque minerals.	

Sample No.	Location	Formation	Rock Name	Microscopic Observation	Remark
2A13	Aït Sáid	Basement Granites	Aplitic Granite (Carapace)	The rock shows granular texture with quartz-ferruginous veins. Main constituent minerals are quartz, orthoclase, plagioclase and two micas. Quartz is anhedral in form and up to 2.0 mm in size. Orthoclase is anhedral and up to 4.0 mm in size. It shows Carlsbad twinning, in part. Most quartz and orthoclase have coexisted and show graphic texture. Plagioclase shows albite twinning and subhedral to anhedral form. It is up to 2.0 mm in length and shows graphic texture with quartz in parts. These minerals are penetrated and crashed by quartz ferrugious veins. The vein is made of very fine grained (0.01 mm) quartz, iron oxidized and a few amount of carbonate. Other constituent minerals are brownish biotite, muscovite and opaque minerals.	Photomicrograph No. 7
2B28	Tamarout	Basement Granites	Aplite	This is glanular in texture and mainly composed of quartz, orthoclase and plagioclase. Anhedral quartz is up to 0.5 mm in size. Orthoclase shows Carlsbad twinning and perthite structure. Some orthoclases are very large crystal (up to 4.0 mm) and subhedral in form. But, most orthoclases are anhedral and about 0.5 mm in length. Plagioclase shows anhedral form and albite twinning (up to 0.3 mm in length). A few amount of biotite occurs in subhedral form and light - dark brown in colour. Other accessary minerals are apatite, zircon and opaque minerals.	Photomicrograph No. 8
2B29	Bou Mia	Basement Granites	Porphyritic Granite	This is granular in texture and composed of quartz, orthoclase, plagioclase and biotite. Anhedral quartz is up to 8.0 mm in size. Anhedral orthoclase shows carlsbad twinning and perthite structure, albite part of which shows albite twinning. It is up to 10.0 mm in length. Anhedral plagioclase shows albite twinning and weak zonal structure, core of which is suffured of sericitization. Biotite is up to 2.0 mm in length and light to dark brown in colour. This is accompained by zircon, apatite and opaque minerals. Zircon shows pleochroic halo. Sphene and muscovite occurs in parts.	

Sample No.	Location	Formation	Rock Name	Microscopic Observation	Remark
2B30	Bou Mia	Basement Granites	Granite Porphyry	The rock shows porphyritic texture. Phenocrysts are composed of quartz, orthoclase and plagioclase. Graundmass is made of the same mineral assemblage, and affected by sericitization and iron-oxidization. Phenocryst quartz is euhedral to subhedral in form (up to 6.0 mm) and shows corroded form. Orthoclase shows euhedral to subhedral and Carlsbad twinning. It is up to 4.0 mm in length. Plagioclase is also euhedral to subhedral and up to 4.0 mm in length. It shows albite twinning and is affected by sericitization. Mafic minerals are perfectly replaced by albite and accompained by sphene and opaque minerals. Groundmass is compossed of felsic minerals and secondary sericite. Felsic minerals are up to 0.2 mm and show micrographic texture.	Photomicrograph No. 9
2B31	Bou Mia	Basement Granites	Granite Porphyry	The rock shows porphyritic texture. Phenocrystic minerals are quartz, orthoclase, a few amount of plagioclase and muscovite. Groundmass is composed of felsic minerals and sericite. Phenocrystic quartz shows subhedral and corroded form (up to 1.5 mm). Orthoclase is subhedral in form and up to 1.5 mm in length. It shows carlsbad twinning. Plagioclase shows albite twinning and subhedral form (up to 1.5 mm). Muscovite is up to 1.0 mm in length. In this rock, there is two type groundmass. One is very fine grained (up to 0.03 mm) felsic minerals and layered sericite. The other is fine -grained (up to 0.2 mm) felsic minerals and dispersed acicular sericite. The latter is nearly same as the above mentioned rock No. 2B30. The boundary of them is sharp. Other accessary minerals are apatite and opaque minerals.	

Sample No.	Location	Formation	Rock Name	Microscopic Observation	Remark
M-001	Zayda Mine No. 54 pit	P-T Red Sandstone	Mineralized Arkose Sandstone	Constituent minerals are quartz, orthoclase, plagioclase, biotite, barite, opaque minerals and clay minerals. Anhedral quartz, up to 4.0 mm, shows wavy extinction. Orthoclase shows carlsbad twinning and perthite structure, up to 4.0 mm in length. Plagioclase which may be oligoclase, shows albite twinning, 0.1 mm - 1.0 mm. Subhedral biotite is dark-brown in colour. Euhedral barite is aggrogatod in lathlike form and shows plumose pattern. The barite, opaque minerals and clay minerals occur like cementation between the original crystals.	Photomicrograph No. 10
M-002	Aśsaka	Basement Granites	Biotite Granite	Constituent minerals are quartz, orthoclase plagioclase, biotite, perthite and opaque minerals. They show granular texture. Anhedral quartz is up to 3.0 mm in length and in places shows graphic texture with orthoclase. Orthoclase shows perthite structure and carlsbad twinning. Plagioclase shows albite twinning and zonal structure. It may be andesine - oligoclase. Subhedral biotite is light brown to brown in colour and up to 2.0 mm in length.	Photomicrograph No. 11
M-003	Boring Core No. 6-12	Basement Granites	Muscovite Granite	It shows granular texture. Anhedral quartz, in places, shows graphic texture with feldspars. Orthoclase shows perthite structure and Carlsbad twinning, up to 0.5 mm in length. Plagioclase (oligoclase) shows albite twinning, and in place, shows intergraphic texture with orthoclase. Subhedral muscovite is up to 0.5 mm in legth, and someplaces is altered to chlorite.	
M-004	Boring Core No. 6-12 36.8 m ~ 37.1 m	P-T Red Sandstone	Hematite bearing Arkose Sandstone	Constituent minerals are fine-grained quartz, orthoclase, muscovite and hematite, Aggregated fine hematite occurs in vein, along which secondary quartz occurs.	
M-005	Boring Core No. 6-12 8 m ~ 15 m	P-T Red Sandstone	Fine-grained Sandstone	Anhedral fine-grained crystals of quartz, orthoclase, plagioclase and muscovite, up to 0.5 mm, are cemented by glass and hematite (limonite). In parts, carbonates occur with hematite.	Photomicrograph No. 12

Sample No.	Location	Formation	Rock Name	Microscopic Observation	Remark
M-006	Aśsaka	Basement Granites	Two Mica Granite	Texture is granular. Quartz is 0.1 - 1.0 mm in length. Orthoclase shows Carlsbad twinning and perthite structure, and has graphic quartz. Plagioclase show albite twinning. Muscovite is colourless and up to 1.0 mm. Biotite is light - dark brown and accompanied by opaque minerals.	
M-007	Aśsaka	Basement Granites	Contaminated Granite	It has xenolith of granite and phenocrysts of quartz and feldspars. Matrix is consisted of fine-grained quartz, feldspars, muscovite and glass. The glass is mostly altered to limonite.	
1A12	Zayda Mine No. 54 pit	P-T Red Sandstone	Pb-ore	Ore minerals and their occurrences are the same as the sample No. M001	Photomicrograph No. 13
1E07	Bou Tsakourt	Basement Granite	Pb-ore	Ore minerals are almost galena and cerrucite. They occure between gangue minerals. Galena is up to 1 m/m in size and its crystal margin is carbonitized and replaced by cerrucite with warmeaten form.	Photomicrograph No. 14
1K31	Sidi Ayyad	Basement Granite	Pb-ore (Marabout vein)	Ore minerals are galena, cerrucite and chalcopyrite. Galena is up to 2 m/m in size and occures with quartz and fluorite. Cerrucite occures in the marginal parts of galena crystals, replacing galena with carbonitization. Chalcopyrite is about 0.03 m/m in size and occuring within galena.	Photomicrograph No. 15
4I05	Anc Mine	J_1 Limestone	Pb-ore	This sample is composed of chalcopyrite, Cu-Fe secondary mineral and gangue minerals. Chalcopyrite is up to 1 m/m in size and occures with gangue minerals, oxidized and replaced by Cu-Fe secondary mineral with worm-eaten form, along the margins and the cleavages of galena crystals.	

(8)

Sample No.	Location	Formation	Rock Name	Microscopic Observation	Remark
4J14	Mibladane	J_1 Limestone	Pb-ore	Ore minerals are composed of galena and cerrucite. Gangue minerals are quartz and dolomite. Galena is carbonitized and replaced by irregular cerrucite and euhedral dolomite, along the margins of galena crystals.	Photomicrograph No. 16
M001	Zayda Mine No. 54 pit	P-T Red Sandstone	Mineralized Arkose, Sandstone	Ore minerals are mostly galena and a little of sphalerite. They occure between gangue minerals. Galena is anhedral and up to 1.0 mm in size. Fine grained and dotted sphalerite occurs in galena crystals.	

Table I—7 Observations of X-ray Microanalysis

Sample No.	Location	Formation	Rock Name	Observation	Remark
1D13	Assaka-n-Tabhirt	Basement Granites	Granite Porphyry	Two uranium minerals are detected in this sample. One is becquerelite $CaO.6UO_3.11H_2O$ recognized in U and Ca X-ray reflective images. The other is carnotite $K_2(VO_2)_3(V_2O_8).3H_2O$ recognized in U and V X-ray reflective images. It is found in U, V and Fe X-ray reflective images that carnotite is occuring with fervanite $2Fe_2O_3.2V_2O_5.5H_2O$. Gangue minerals are silicate and iron oxide minerals.	U:0,139% 1,000c/s
1D15	Paneau-1	P-T Red Sandstone	Arkose Sandstone	No uranium mineral is detected in this sample. There is found the following minerals cementing between fragments consisting of arkose sandstone. Barite ; in Ba and S X-ray reflective images. Fluorite: in Ca X-ray reflective image Hematite: Showing strong reflection in Fe X-ray reflective image.	U:0,061% 7,000c/s
1K08	Sidi Ayyad		Fe-quartz Vein	Carnotite, composed of U, V and K, is detected in this sample. It is evident in Fe, V, Si and Ca X-ray reflective images that carnotite is occured within the margin of altered fervanite crystal. Gangue minerals are K-Al silicate and Fe-Al silicate.	U:0.188% 2,000c/s
2A13	Aït Sáid	Basement Granite	Aplitic Granite (carapace)	Carnotite is found in U, V and K X-ray reflective images. It is presumed in this sample that there is tyuyamunite $Ca(VO_2)_2(V_2O_8).5H_2O$ replaced K, in carnotite, to Ca. Gangue mineral is ferrouginous quartz consisted of silica and iron oxide.	U:0,072% 1.600c/s

Table I—8 Photomicrographs

Abbreviation

Ba	:	Barite
Bio	:	Biotite
Car	:	Carnotite
Ccp	:	Chalcopyrite
Ce	:	Cerusite
Chl	:	Chlorite
Dol	:	Dolomite
Fe	:	Fe-oxide
Fl	:	Fluorite
G	:	Gangue mineral
Gn	:	Galena
Gr	:	Groundmass
Hb	:	Hornblende
Ht	:	Hematite
Opq	:	Opaque mineral
Or	:	Orthoclase
Pl	:	Plagioclase
Q	:	Quartz
Sp	:	Sphalerite
V	:	Vein

1

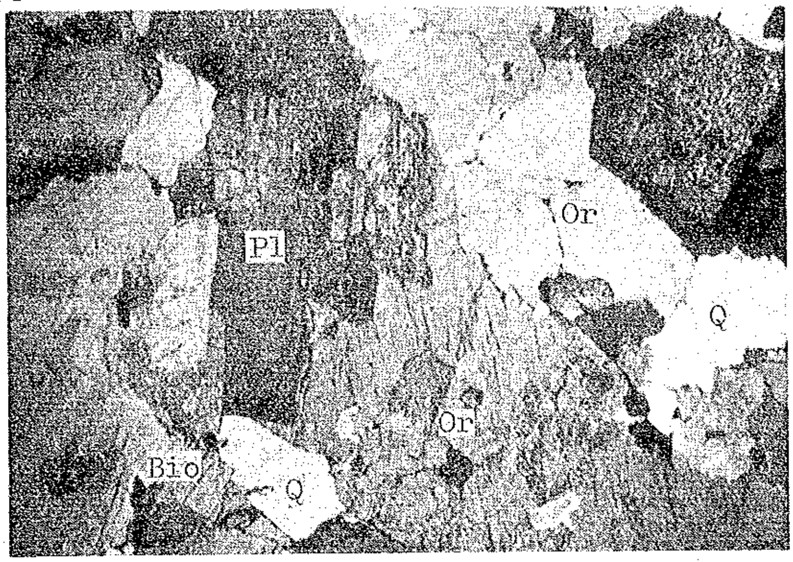

Sample No. 1B04 — 1mm — Crossed nicols

Rock name: Contaminated granite

2

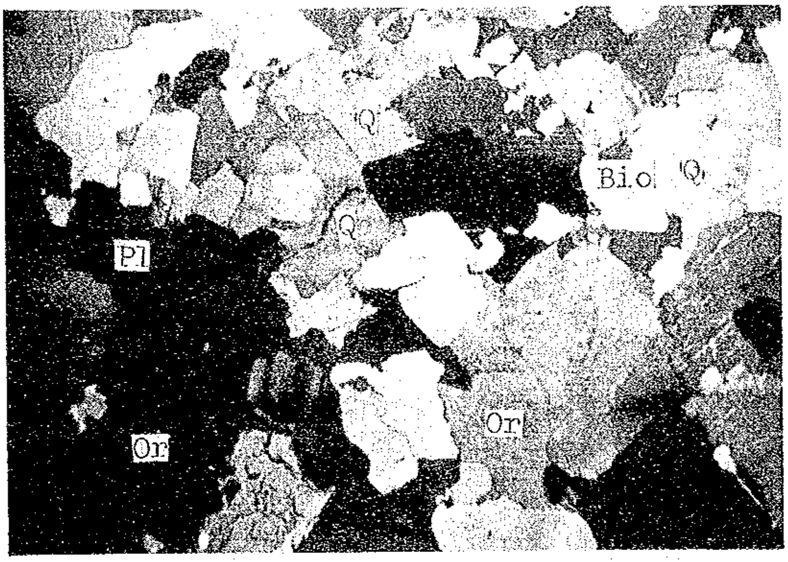

Sample No. 1B05 — 1mm — Crossed nicols

Rock name: Aplitic granite

3

Sample No. 1D15 — 1mm

Rock name: Arkose sandstone — Crossed nicols

4

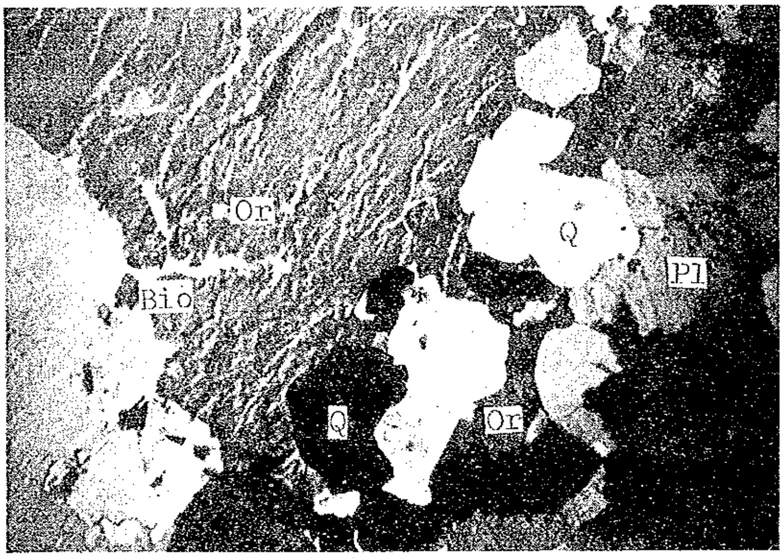

Sample No. 1D20 — 2 mm

Rock name: Porphyritic granite — Crossed nicols

5

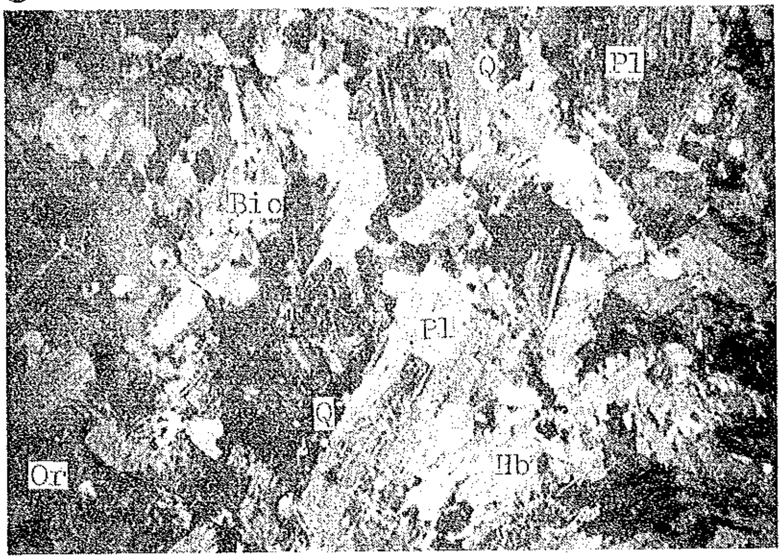

Sample No. 1K09

1 mm

Crossed nicols

Rock name: Granodiorite

6

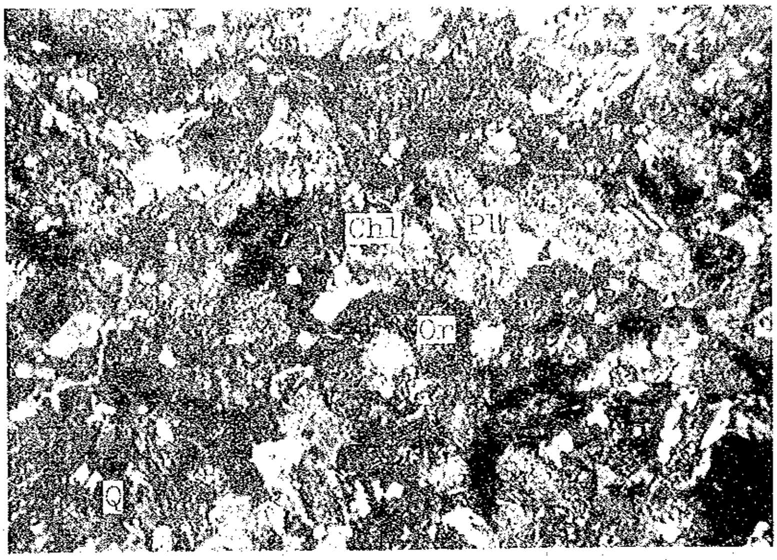

Sample No. 1K22

0.4 mm

Crossed nicols

Rock name: Microgranodiorite

7

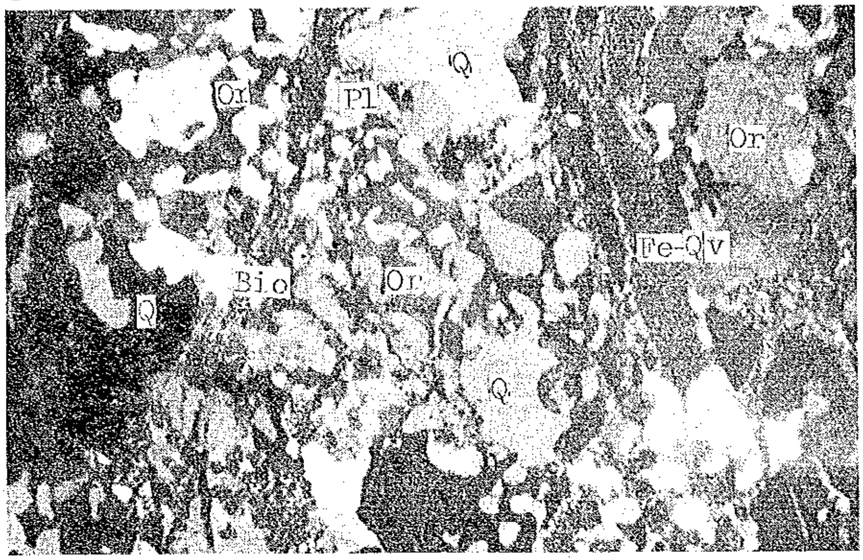

Sample No. 2A13

2 mm

Crossed nicols

Rock name: Aplitic granite
(with graphic texture)
(carapace)

8

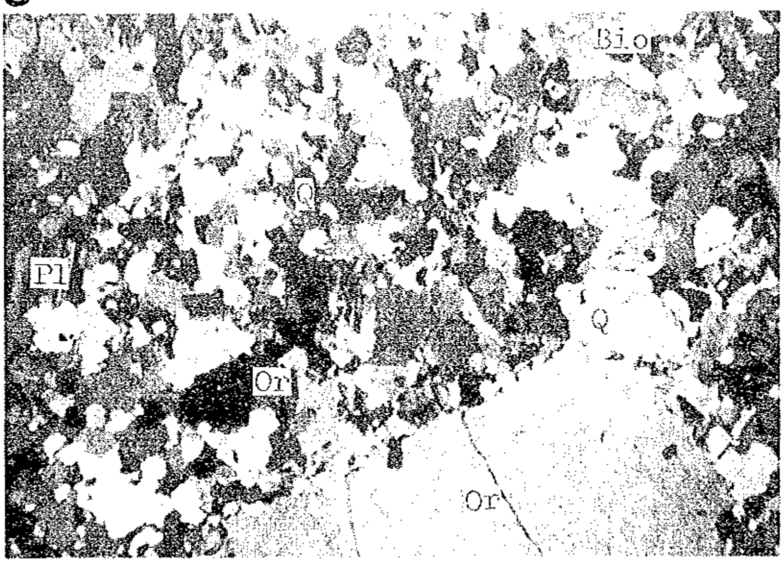

Sample No. 2B28

1 mm

Crossed nicols

Rock name: Aplite

9

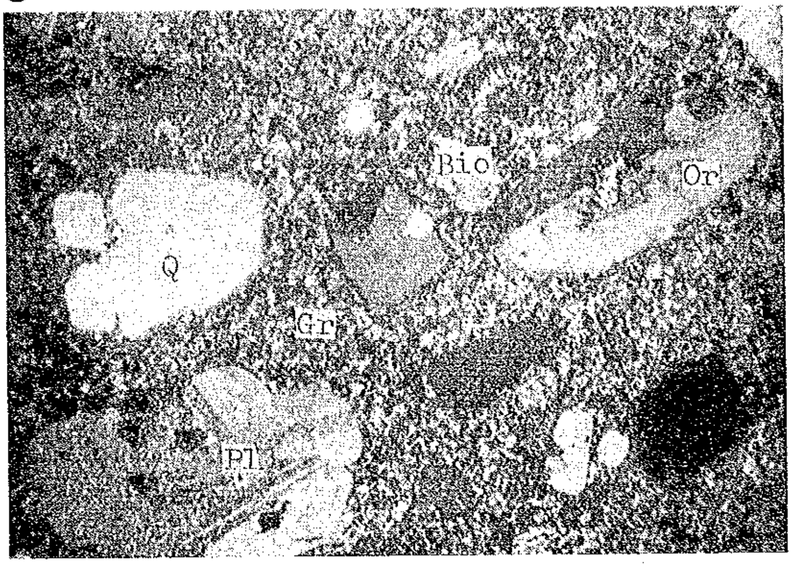

Sample No. 2B30

1 mm

Crossed nicols

Rock name: Granite porphyry

10

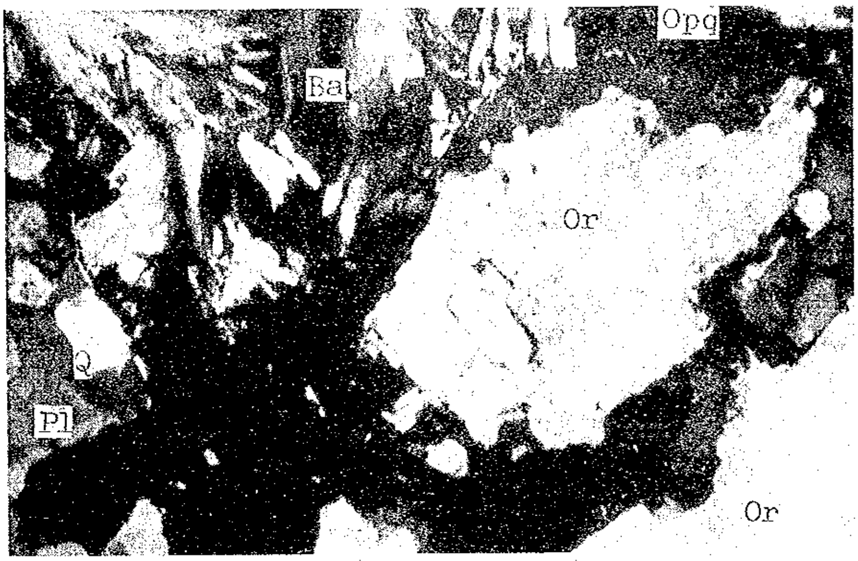

Sample No. M001

1 mm

Crossed nicols

Rock name: Mineralized arkose sandstone

11

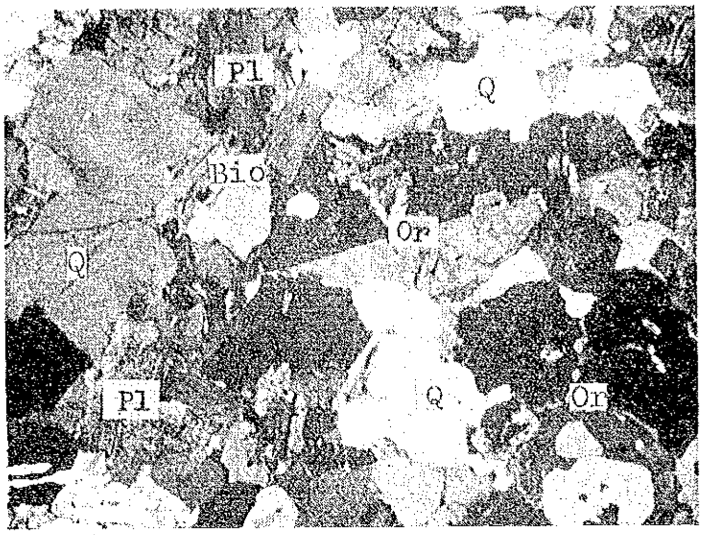

Sample No. M002

2 mm

Crossed nicols

Rock name: Biotite granite

12

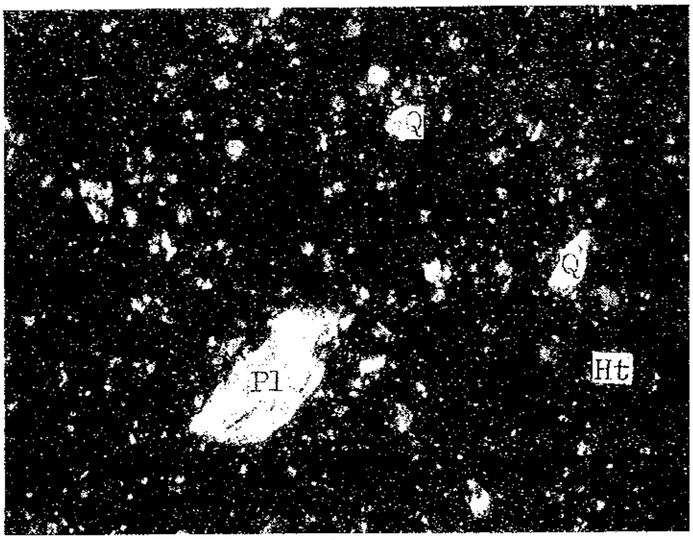

Sample No. M005

1 mm

Crossed nicols

Rock name: Fine-grained sandstone

13

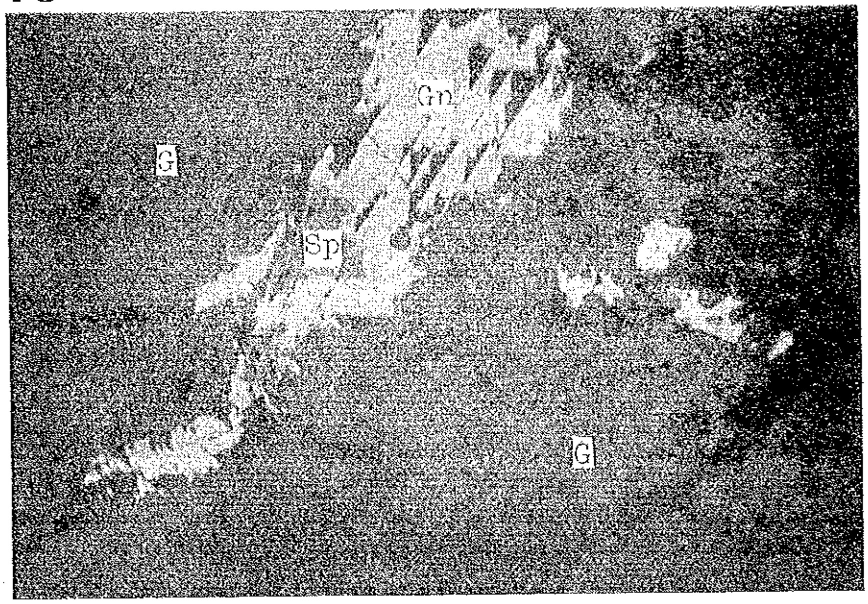

Sample No. 1A12

0.2 mm

Crossed nicols

Rock name: Pb-ore (Zayda pit No.54)

14

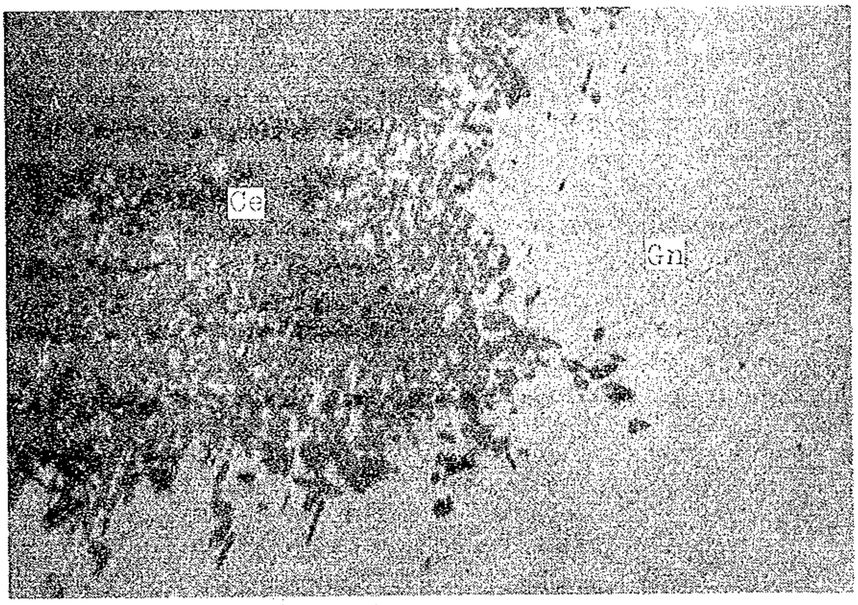

Sample No. 1E07

0.2 mm

Crossed nicols

Rock name: Pb-ore (Bou Tsakourt)

15

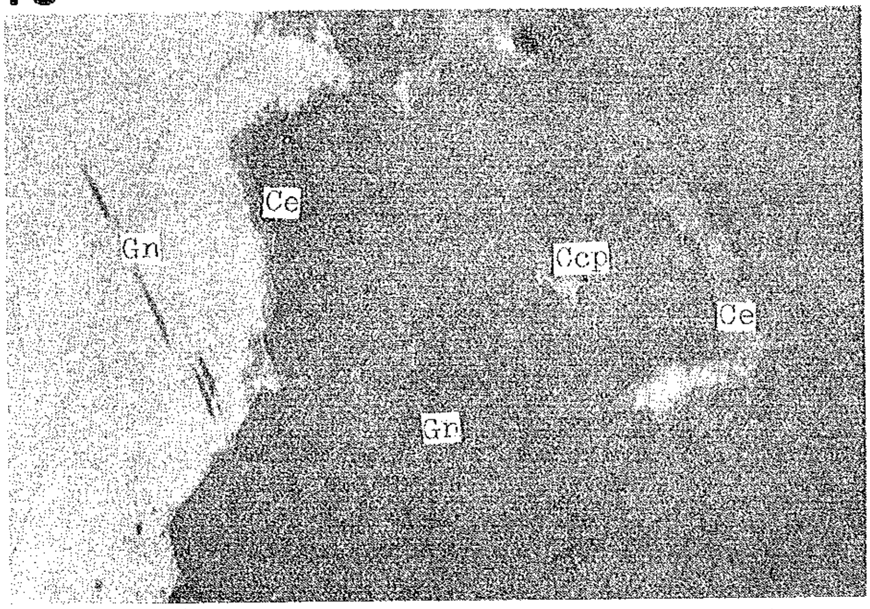

Sample No. 1K31

0.2 mm

Crossed nicols

Rock name: Pb-ore (Sidi Ayyad)

16

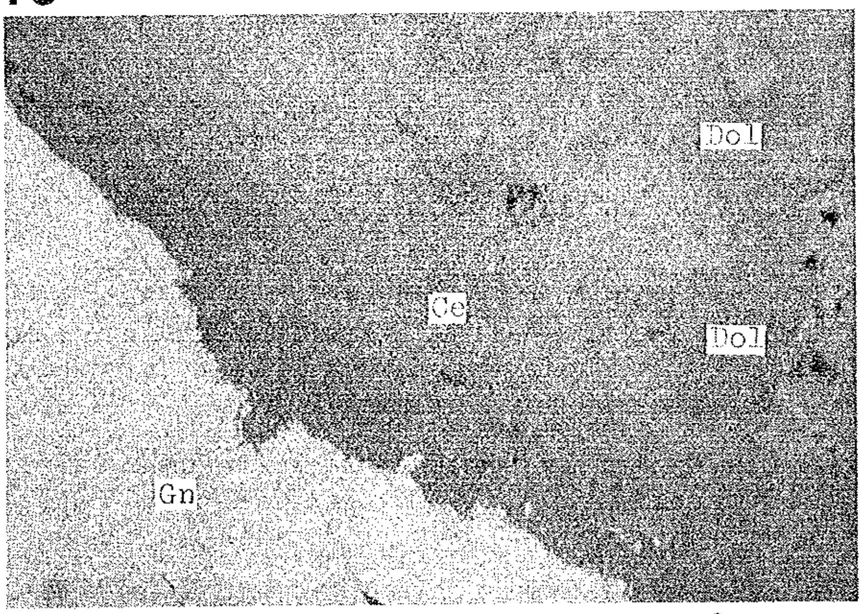

Sample No. 4J14

0.2 mm

Crossed nicols

Rock name: Pb-ore (Mibladane "L" pit)

17

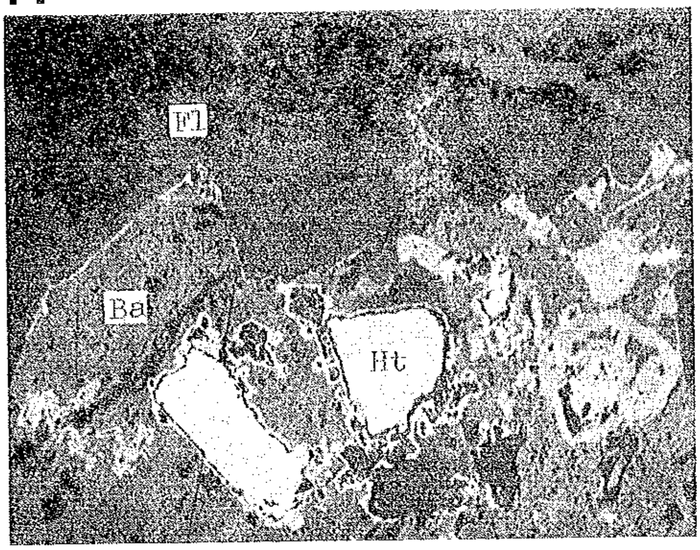

Sample No. 1D15

0.2 mm

Crossed nicols

Rock name: Arkose sandstone

18

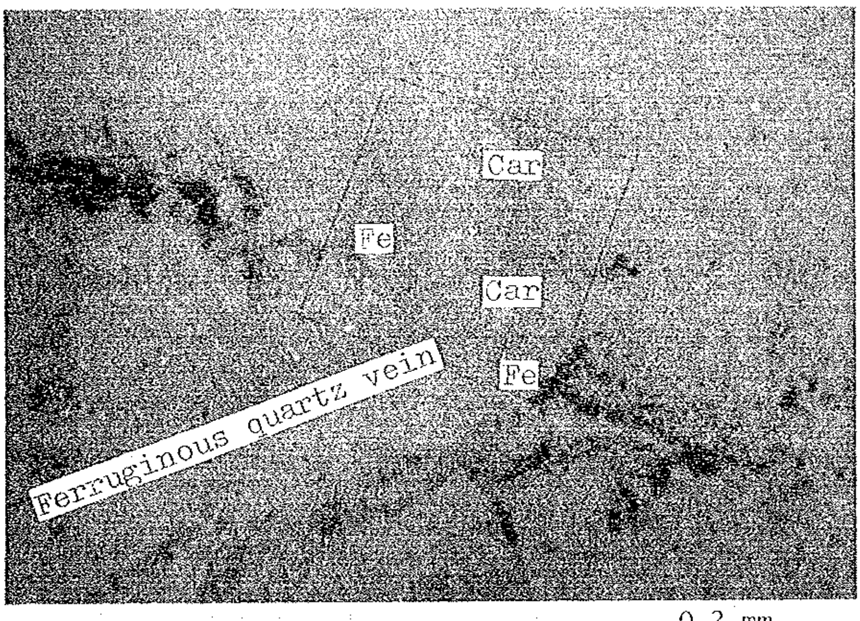

Sample No. 2A13

0.2 mm

Crossed nicols

Rock name: Aplitic granite
(carapace)